RNA preparation and DNA microarray analysis. Total RNA was extracted from ovarian cancer cells by the acid guanidinium method and was subjected to a synthesis of double-stranded cDNA with oligo-dT primer, which was then used to prepare biotin-labeled cRNA with the use of the GeneChip labeling system (Affymetrix, Santa Clara, CA, USA). The resultant cRNA was then hybridized to GeneChip HGU95Av2 microarray (Affymetrix) revealing the expression intensities of 12,625 probe sets in each sample. Detection of hybridization signals and the statistical analyses of the digitized data were performed with a GMS 418 array scanner (Affymetrix) and Gene Spring 3.2.2 software (Silicon Genetics, Redwood, CA, USA), respectively. The fluorescence intensity for each gene was normalized relative to the median fluorescence value for all human genes with a 'Present' or 'Marginal' call (Microarray Suite; Affymetrix) in each hybridization. In the hierarchical clustering analysis, similarity was measured by the Pearson's correlation with a separation ratio of 1.0. The details of the genes shown in the figures are available upon request.

Real-time reverse transcription-polymerase chain reaction (RT-PCR) analysis. To verify the data obtained from microarrays, we carried out real-time RT-PCR analysis. Portions of unamplified cDNA were subjected to PCR with SYBR-Green PCR Core Reagents (PE Applied Biosystems, Foster City, CA, USA). The incorporation of the SYBR-Green dye into the PCR products was monitored in real-time with an ABI PRISM 7700 sequence detection system (PE Applied Biosystems), thereby allowing determination of the threshold cycle (Ct) at which exponential amplification of PCR products begins. The Ct values for cDNAs corresponded to the GAPDH gene and target transcripts relative to that of GAPDH mRNA. The oligonucleotide primers for PCR were as follows: GAPDH cDNA, 5'-CGCGGGGCTCTCAGAACATCAT-3' and 5'-CCAGCCCCAGCGTCAAAGGTG-3'; glutathione peroxidase 3 (GPX 3) cDNA, 5'-AGCAGTATGCTGGCAA ATATGTCC-3' and 5'-CAGACCGAATGGTGCAAGCTC TTC-3'.

Selection of short hairpin RNA stable cell lines. The DNA oligonucleotides, encoding short hairpin RNA (shRNA) targeting the GPX3 (forward; CACCGGGAGAGTTTGCAC TATTAACGTGTGCTGTCCGTTAATGGTGCAAGCTCT TCCTTTTT, reverse; GCATAAAAAGGAAGAGCTTGCA CCATTAACGGACAGCACACGTTAATAGTGCAAACTC TCCC) were synthesized, annealed, and cloned into the *Bsp*MI site of the vector piGENE PURhU6 (13), which contains a human U6 promoter and a puromycin resistance gene. The shRNA expression plasmid (piGENE PURhU6/shGPX3) and the control plasmid (piGENE PURhU6) were transfected into four ovarian clear cell carcinoma cell lines by the standard calcium phosphate precipitation method (14). The cells were selected with the concentration of 1 μg/ml puromycin (Calbiochem, Darmstadt, Germany). Resistant clones were obtained after four weeks. The cells were subsequently maintained in the presence of 1 μg/ml puromycin.

Semiquantitative RT-PCR analysis. Using a semiquantitative RT-PCR method, we assessed transcription levels of GPX3 and GAPDH in the transfectants. Total RNAs were extracted from the transfectants by the acid guanidinium method and reverse-transcribed using Reverse Transcription System (Promega, Madison, WI). Each RT-PCR reaction consisted of 25 cycles of 30 sec at 94˚C, 30 sec at 55˚C and 1 min at 72˚C. Amplification of GAPDH revealed similar signal strengths in all samples, as a control for the integrity of each RNA template. PCR products were electrophoresed in 1.5% agarose gels. Primers used for amplification were described above.

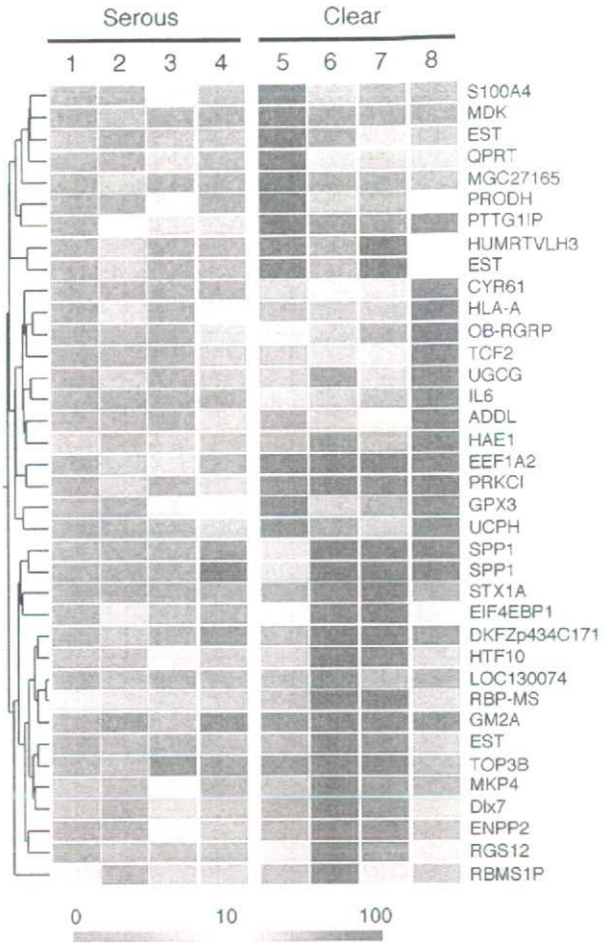

Figure 1. Identification of clear cell adenocarcinoma-specific genes. Hierarchical clustering of 34 probe sets were performed on the basis of their expression profiles in serous adenocarcinoma cell lines [HRA (1), KF (2), KOC-2S (3) and SHIN-3 (4)] and clear cell adenocarcinoma cell lines [KK (5), OVMANA (6), OVSAYO (7) and RMG1 (8)]. Each column represents a separate cell line and each row a single probe set on the microarray. Expression level of each probe set is shown color-coded as indicated by the scale at the bottom. Note that two distinct probe sets are assigned to the *PP1* gene on GeneChip HGU95Av2 array.

Colorimetric assay. The sensitivity of the transfectants to cisplatin (Bristol-Myers Squibb Co., Ltd., Tokyo, Japan) was investigated by colorimetric assay using Cell Proliferation kit II (XTT) (Boehringer Mannheim GmbH Biochemica, Mannheim, Germany). The transfectants were exposed to cisplatin at concentrations of 1-128 μM for 24 h. The viable cell count measured by colorimetric assay was presented as a percent ratio to the count of the control untreated with cisplatin. A

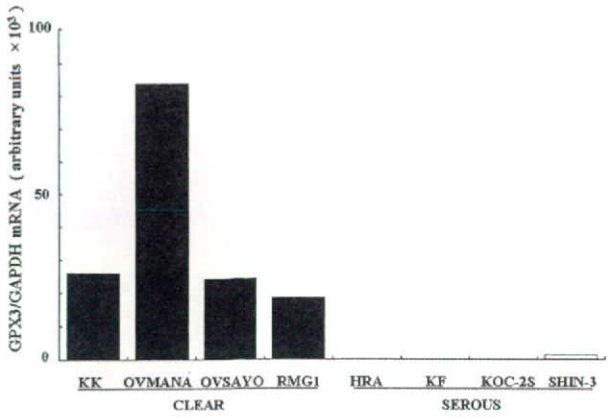

Figure 2. Quantitation of *GPX3* transcripts in ovarian cancer cell lines. Complementary DNA prepared from the ovarian cancer cells was subjected to real-time RT-PCR with primers specific for *GPX3* or *GAPDH* genes. The ratio of the abundance of the *GPX3* transcript to that of GAPDH mRNA was calculated as 2^n, where n is the Ct value for *GAPDH* cDNA minus the Ct value of the *GPX3* cDNA.

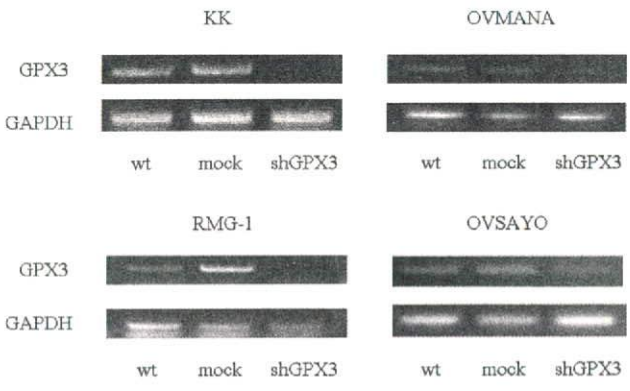

Figure 3. Expression of GPX3 in clear cell adenocarcinoma transfectants. GPX3 expression by the semiquantitative RT-PCR method was decreased in cells transfected with the shRNA expression plasmid in all 4 clear cell adenocarcinoma cell lines compared with the parent and control cell lines. The integrity of each RNA template was controlled through amplification of GAPDH.

dose-response curve was prepared and the 50% growth inhibitory concentration (IC_{50}) was obtained for cisplatin.

Results

DNA microarray analysis. Expression intensities of >12,000 human probe sets were examined in a total of 8 samples. To identify genes whose expression was specific to the clear cell adenocarcinoma subtype, we first calculated the mean expression levels of each gene in both clear cell adenocarcinoma and serous adenocarcinoma group. With the use of GeneSpring software, we then searched for genes whose expression profiles were similar, with a minimal correlation of 0.99, to that of a hypothetical 'clear cell adenocarcinoma-specific gene' with a mean expression level of 0.0 arbitrary unit (U) in the serous adenocarcinoma and of 200.0 U in the clear cell adenocarcinoma. From the resulting genes, we then selected those whose expression level was ≥60.0 U in at least one of the clear cell adenocarcinoma group. A total of 34 probe sets (corresponding to 33 human genes) were finally identified to be specific to the clear cell adenocarcinoma cell lines, including those for secreted phosphoprotein 1 (SPP1), eukaryotic translation elongation factor 1α2 (EEF1A2), hereditary angioedema (HAE) 1, pituitary tumor-transforming gene 1 (PTTG1IP), UDP-glucose ceramide glucosyltransferase (UGCG) and GPX3.

Table I. IC_{50} value (μM) and sensitivity index for cisplatin in the 4 types of clear cell adenocarcinoma transfectants.

	IC_{50} (μM)	Sensitive index
KK/mock	25.0±0.5	-
KK/shGPX3	7.5±0.9	3.3
OVMANA/mock	54.9±2.0	-
OVMANA/shGPX3	13.9±0.5	4.0
RMG-1/mock	54.7±4.4	-
RMG-1/shGPX3	12.9±0.3	4.2
OVSAYO/mock	26.6±0.4	-
OVSAYO/shGPX3	24.5±2.5	1.1

Expression profiles of these clear cell adenocarcinoma-specific genes were shown as a dendrogram, or 'gene tree,' in which genes with similar expression profiles among the samples were clustered near each other (Fig. 1).

Real-time reverse transcription-polymerase chain reaction (RT-PCR) analysis. To confirm the group-specific expression of these genes, we measured their mRNA level by the quantitative real-time RT-PCR method. As shown in Fig. 2, the relative expression level of *GPX3* to *GAPDH* was, for instance, highly induced in the clear cell adenocarcinoma cell lines, but negligible in the serous adenocarcinoma cell lines.

Expression of GPX3 in clear cell adenocarcinoma transfectants. As shown in Fig. 3, GPX3 expression by the semiquantitative RT-PCR method decreased in cells transfected with the shRNA expression plasmid in all 4 clear cell carcinoma cell lines compared with the parent and control lines. The integrity of each RNA template was controlled through GAPDH amplification.

Cisplatin sensitivity. The dose-response curves of the 4 types of clear cell adenocarcinoma transfectants to cisplatin are shown in Fig. 4 and the IC_{50} values (μM) in Table I. The ratio of the IC_{50} value in cells transfected with the shRNA expression plasmid to that in the control cells was defined as the sensitivity index. In KK, OVMANA, and RMG-1, the sensitivity index was 3.3, 4.0 and 4.2, respectively, showing an increase in cisplatin sensitivity by the suppression of GPX3 expression. In OVSAYO, the sensitivity index was 1.1, showing no definite change.

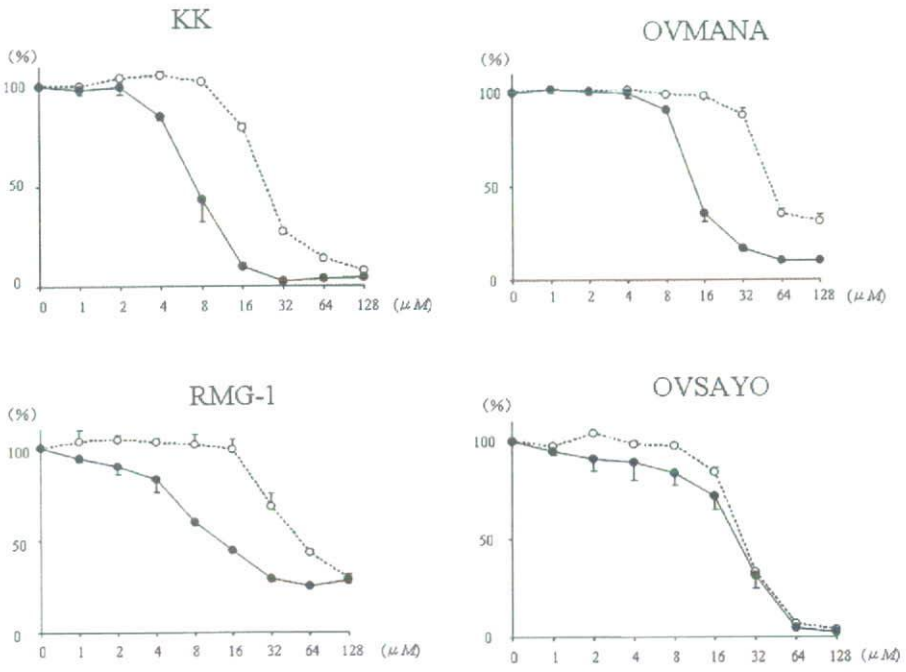

Figure 4. Dose-response curves of the 4 types of clear cell adenocarcinoma transfectants to cisplatin. Open circle, control cells; solid circle, cells transfected with the shRNA expression plasmid. The average of three independent experiments is shown and error bars indicate SD.

Discussion

Among the 33 genes that were up-regulated in the clear cell adenocarcinoma cell lines, SPP1 has been reported to be involved in bone metabolism, EEF1A2 in the repair of DNA damage in lymphoid cells, HAE1 in hereditary angioedema (as the responsible gene), PTTG1IP in the development of pituitary tumor and UGCG in the biosynthesis of glycosphingolipids.

GPX3 is an oxygen radical-metabolizing enzyme. Since GPX3 functions in the detoxification mechanisms of various substances (15,16), it was interesting to find *GPX3* in the specific genes to clear cell adenocarcinoma which is a chemoresistant malignancy. Studying clinical specimens of ovarian cancer, Hough *et al* (17) reported that *GPX3* was up-regulated in clear cell adenocarcinoma, similar to the results of our study. Thus, analyses of both cell lines and fresh clinical specimens have indicated that the up-regulation of the *GPX3* gene may be one of the molecular characteristics of clear cell adenocarcinoma.

GPX3 suppression by RNA interference definitely increased cisplatin sensitivity in 3 of the 4 clear cell adenocarcinoma cell lines. This experiment showed that GPX3 is involved in cisplatin sensitivity, suggesting that low cisplatin sensitivity is due to high GPX3 expression in clear cell adenocarcinoma, which in many cases highly expresses GPX3 (17).

For the anticancer drug resistance mechanism of cancer cells, promotion of excretion of anticancer drugs from cells, promotion of DNA repair and inhibition of apoptosis are generally considered. Previous study reports of anticancer drug resistance of clear cell adenocarcinoma, particularly cisplatin resistance, are discussed below.

Multidrug resistance-associated protein (MRP) and P-glycoprotein (P-gp) excrete anticancer drugs from cells in a ATP-dependent manner and decrease intracellular accumulation of anticancer drugs and are closely associated with multidrug resistance of various cancers. However, according to Itamochi *et al*, MPR or P-pg expression was not related to cisplatin sensitivity in clear cell adenocarcinoma either *in vitro* or clinical cases (4).

There is almost no previous data on DNA repair system in clear cell adenocarcinoma. Only Reed *et al* reported that ERCC1 and XPB associated with DNA repair were highly expressed in clear cell adenocarcinoma (18). However, an increase in DNA repair in clear cell adenocarcinoma has not been directly demonstrated.

Tsuchiya *et al* found a new candidate gene associated with anticancer drug resistance of clear cell adenocarcinoma (19). They nominated hepatocyte nuclear factor-1ß (HNF-1ß) for the candidate gene based on DNA microarray analysis of 4 clear cell adenocarcinoma cell lines. They suggested that *HNF-1β* is a gene involved in the low sensitivity, based on the findings that HNF-1ß was highly expressed in many patients with clear cell adenocarcinoma and inhibition of HNF-1ß expression induced apoptosis of clear cell adenocarcinoma cells *in vitro*. Although association of *HNF-1β* gene with low cisplatin sensitivity was not directly demonstrated, this is an interesting study.

In summary, we identified *GPX3* as a gene highly expressed in clear cell adenocarcinoma by DNA microarray and real-time RT-PCR. GPX3 suppression by RNA interference increased the cisplatin sensitivity of clear cell adenocarcinoma cells. *GPX3* was suggested to be a candidate gene associated with low cisplatin sensitivity of clear cell adenocarcinoma.

References

1. Jemal A, Murray T, Ward E, *et al*: Cancer statistics, 2005. CA Cancer J Clin 55: 10-30, 2005.
2. Sugiyama T, Kamura T, Kigawa J, *et al*: Clinical characteristics of clear cell carcinoma of the ovary: a distinct histologic type with poor prognosis and resistance to platinum-based chemotherapy. Cancer 88: 2584-2589, 2000.
3. Goff BA, Sainz de la Cuesta R, Muntz HG, *et al*: Clear cell carcinoma of the ovary: a distinct histologic type with poor prognosis and resistance to platinum-based chemotherapy in stage III disease. Gynecol Oncol 60: 412-417, 1996.
4. Itamochi H, Kigawa J, Akeshima R, *et al*: Mechanisms of cisplatin resistance in clear cell carcinoma of the ovary. Oncology 62: 349-353, 2002.
5. Itamochi H, Kigawa J, Sugiyama T, *et al*: Low proliferation activity may be associated with chemoresistance in clear cell carcinoma of the ovary. Obstet Gynecol 100: 281-287, 2002.
6. Kikuchi Y, Hirata J, Kita T, *et al*: Enhancement of anti-proliferation effect of cis-diamminedichloroplatinum(II) by clomiphene and tamoxifen in human ovarian cancer cells. Gynecol Oncol 49: 365-372, 1993.
7. Yanagibashi T, Gorai I, Nakazawa T, *et al*: Complexity of expression of the intermediate filaments of six new human ovarian carcinoma cell lines: new expression of cytokeratin 20. Br J Cancer 76: 829-835, 1997.
8. Kiguchi K, Iwamori M, Mochizuki Y, *et al*: Selection of human ovarian carcinoma cells with high dissemination potential by repeated passage of the cells in vivo into nude mice, and involvement of Le^X -determinant in the dissemination potential. Jpn J Cancer Res 89: 923-932, 1998.
9. Kikuchi Y, Kizawa I and Kato K: Effects of calmodulin antagonists on human ovarian cancer cell proliferation in vitro. Biochem Biophys Res Commun 123: 385-392, 1984.
10. Kikuchi Y, Kizawa I, Oomori K, *et al*: Establishment of a human ovarian cancer cell line capable of forming ascites in nude mice and effects of tranexamic acid on cell proliferation and ascites formation. Cancer Res 47: 592-596, 1987.
11. Imai S, Kiyozuka Y, Maeda H, Noda T and Hosick HL: Establishment and characterization of a human ovarian serous cystadenocarcinoma cell line that produces the tumor markers CA-125 and tissue polypeptide antigen. Oncology 47: 177-184, 1990.
12. Kataoka A, Yokota D, Yakushiji M and Kojiro M: Establishment and characterization of ovarian serous adenocarcinoma cell line (KOC-2S). Hum Cell 1: 337, 1988 (in Japanese).
13. Miyagishi M and Taira K: Strategies for generation of an siRNA expression library directed against the human genome. Oligonucleotides 13: 325-333, 2003.
14. Wigler M, Pellicer A, Silverstein S and Axel R: Biochemical transfer of single-copy eucaryotic genes using total cellular DNA as donor. Cell 14: 725-731, 1978.
15. Kong Q and Lillehei KO: Antioxidant inhibitors for cancer therapy. Med Hypotheses 51: 405-409, 1998.
16. Lelkes PI, Hahn KL, Sukovich DA, Karmiol S and Schmidt DH: On the possible role of reactive oxygen species in angiogenesis. Adv Exp Med Biol 454: 295-310, 1998.
17. Hough CD, Cho KR, Zonderman AB, Schwartz DR and Morin PJ: Coodinary up-regulated genes in ovarian cancer. Cancer Res 61: 3869-3876, 2001.
18. Reed E, Yu JJ, Davies A, Gannon J and Armentrout SL: Clear cell tumors have higher mRNA levels of ERCC1 and XPB than other histological types of epithelial ovarian cancer. Clin Cancer Res 9: 5299-5305, 2003.
19. Tsuchiya A, Sakamoto M, Yasuda J, *et al*: Expression profiling in ovarian clear cell carcinoma: identification of hepatocyte nuclear factor-1 beta as a molecular marker and a possible molecular target for therapy of ovarian clear cell carcinoma. Am J Pathol 163: 2503-2512, 2003.

Autocrine and/or paracrine growth of aggressive ATLL cells caused by HGF and c-Met

Y. ONIMARU[1], K. TSUKASAKI[1], K. MURATA[5], Y. IMAIZUMI[1], Y.L. CHOI[6], H. HASEGAWA[3], K. SUGAHARA[3], Y. YAMADA[3], T. HAYASHI[7], M. NAKASHIMA[2], T. TAGUCHI[4], H. MANO[6], S. KAMIHIRA[3] and M. TOMONAGA[1]

[1]Department of Hematology and Molecular Medicine, [2]Division of Scientific Data Registry, Atomic Bomb Disease Institute, Departments of [3]Laboratory Medicine, and [4]Pathology, Nagasaki University Graduate School of Biomedical Sciences, Nagasaki; [5]Division of Hematology/Clinical Laboratory Medicine, Tottori University, Yonago, Tottori; [6]Division of Functional Genomics, Jichi Medical University, Shimotsukeshi, Tochigi; [7]Department of Pathology, Nagasaki University Hospital, Nagasaki, Japan

Received April 14, 2008; Accepted June 20, 2008

DOI: 10.3892/ijo_00000055

Abstract. Adult T-cell leukemia/lymphoma (ATLL) is a neoplasia characterized by the massive invasion of various organs by tumor cells. Previously, we found that expression of the gene for c-Met, a receptor tyrosine kinase for hepatocyte growth factor (HGF), was specific to the acute type among 41 patients with ATLL by microarray. First in the present study, we analyzed the survival of the patients in relation to expression of c-Met and HGF in ATLL cells. Expression of the former but not the latter was associated with poor prognosis. Then, we analyzed the growth of ATLL cells caused by HGF and c-Met. c-Met was expressed in 0/7 chronic ATLLs, 12/14 acute ATLLs, 1/1 IL-2-independent ATLL cell line and 1/7 IL-2-dependent ATLL cell lines as assessed by flow cytometry. HGF induced the proliferation of primary cells from most acute cases examined as well as the c-Met-positive KK1 cell line in contrast to c-Met-negative cells. HGF induced autophosphorylation of c-Met in c-Met-positive cells from an acute case and KK1 cells. The plasma level of HGF was elevated in acute as compared to chronic cases. The levels of HGF and/or IL-6 which induces the production of HGF by stromal cells, were elevated in the supernatant of short-term cultured cells from certain patients with acute or chronic disease. Finally, infiltrated ATLL cells and adjacent stromal cells in liver were shown to be positive for c-Met/HGF and HGF, respectively, in acute cases. Autocrine and/or paracrine growth caused by HGF and c-Met was suggested in aggressive ATLL cells secreting HGF and/or IL-6, respectively.

Correspondence to: Dr Kunihiro Tsukasaki, Department of Molecular Medicine and Hematology, Molecular Medicine Unit, Atomic Bomb Disease Institute, Nagasaki University Graduate School of Biomedical Science, 1-12-4 Sakamoto, Nagasaki 852-8523, Japan
E-mail: tsukasak@net.nagasaki-u.as.jp

Key words: adult T-cell leukemia/lymphoma, human T-lymphotropic virus type-I, c-Met, hepatocyte growth factor, autocrine/paracrine

Introduction

Adult T-cell leukemia/lymphoma (ATLL) is a distinct peripheral T-lymphocytic malignancy associated with human T-cell lymphotropic virus type-I (HTLV-1) (1-3). The diverse clinical features and prognosis of this disease have led to its subclassification; acute, lymphoma, chronic, and smoldering types (4). Patients with indolent ATLL, i.e. the chronic or smoldering type, have been treated as a subtype of chronic lymphoid leukemia with a watchful-waiting policy until disease progression (5-7). Aggressive ATLL generally has a very poor prognosis as compared to aggressive B-cell lymphoma and peripheral T-cell lymphoma excluding ATLL because of the multidrug-resistance of malignant cells, a large tumor burden with multi-organ failure, hypercalcemia and/or frequent infectious complications due to a profound T-cell immunodeficiency (5-7).

Hepatocyte growth factor (HGF), also known as scatter factor, was identified as a chemoattractant for a variety of cells. HGF is produced by cells of mesenchymal origin, but not by epithelial cells and has a pleiotropic function, such as liver regeneration. It also has mitogenic, morphogenic, and motogenic effects on epithelial cells, as well as endothelial cells (8). The receptor for HGF is encoded by the met proto-oncogene (c-Met). The c-Met protein is a tyrosine kinase cell surface receptor and consists of an extracellular α- and a transmembrane ß chain. The ß chain contains the tyrosine kinase domain as well as the site for tyrosine autophosphorylation. Ligation of HGF causes autophosphorylation of c-Met, followed by a variety of signaling cascades (9). Although normal HGF/c-Met signaling is involved in many aspects of embryogenesis, abnormal HGF/c-Met signaling has been implicated in tumor development and progression

(10,11). In particular, HGF/c-Met signaling has been shown to play a significant role in promoting tumor cell invasion and metastasis. Furthermore, HGF and/or c-Met expression/overexpression has been documented in a wide variety of human tumors (10,11). c-Met is predominantly expressed in epithelial cells but has been detected in various hematopoietic cells as well (12). Furthermore, lymphoid malignancies, such as multiple myeloma and several B cell lymphomas, were found to express c-Met, suggesting that c-Met is involved in the pathogenesis of these diseases (13,14).

We have reported frequent hepatic involvement and the relationship between liver invasion and poor prognosis in ATLL, and the relationship was associated with c-Met expression on ATLL cells (15,16). Recently, using microarray-based gene expression profiling, we performed a comprehensive genomic analysis of ATLL in order to investigate the mechanism of progression from chronic to acute disease, and found that c-Met expression was shown to be specific to acute type ATLL and the plasma concentration of HGF was increased in some individuals with acute or chronic type ATLL (17).

To clarify the interaction of c-Met/HGF in the multistep leukemogenesis and tissue-invasiveness of ATLL, we investigated the possible autocrine/paracrine loop using ATLL cell lines, and primary leukemic cells and liver autopsy specimens from patients with the disease.

Materials and methods

Clinical and microarray data for analyzing the relationship of prognosis and c-Met/HGF expression in ATLL. Isolated $CD4^+$ leukemic cells from cases of the chronic (n=19) or acute (n=22) ATLL had been subjected to profiling of gene expression with oligonucleotide microarrays containing >44,000 probe sets including those for c-Met and HGF in our previous study (17). Collected clinical data for each patient were correlated with the expression data in this study.

Cell lines. Eight HTLV-I-positive T-cell lines were used. Six of the 7 cell lines established by us, SO4, ST1, KK1, KOB, LMY-1 and LMY2 excluding OMT, were each derived from a primary ATLL clone confirmed by Southern blotting for HTLV-1-integrated sites. The origin of HUT102 is unknown. HUT102, an interleukin (IL)-2-independent cell line, was grown in RPMI-1640 medium supplemented with 10% heat-inactivated FBS, penicillin G (50 units/ml), and streptomycin (50 μg/ml) in a humidified incubator containing 5% CO_2 in air. The other 7 cell lines were IL-2-dependent, and were grown in a medium identical to that for HUT102 with 200 Japan reference units (JRUs)/ml recombinant IL-2 (provided by Takeda Chemical Industries, Osaka, Japan).

Patient samples for analyzing the growth of ATLL cells caused by HGF and c-Met. We assessed 21 patients with ATLL, 14 and 7 with acute and chronic types, respectively, having >90% ATLL cells phenotypically confirmed by more than two parameters among CD2, CD3, CD4, CD5 and CD25 in peripheral blood mononuclear cells (PBMNCs). Four out of the 21 patients (3 acute types and 1 chronic type) were included in our previous study (17). The diagnosis of ATLL was based on clinical features, hematological findings including cytologically or histologically proven mature T-cell leukemia/lymphoma, and serum anti-HTLV-I antibodies (16,17). Integration of the monoclonal HTLV-I provirus into the genomic DNA of malignant cells was confirmed by Southern blot hybridization in all cases. PBMNC and plasma from patients with ATLL were obtained by density gradient separation from peripheral blood, before chemotherapy, with informed consent. PBMNCs and plasma were also obtained from healthy individuals.

Detection of c-Met protein on the cell surface by flow cytometric analysis. The expression of c-Met on the cell surface was analyzed by flow cytometry as described (17). Briefly, 3-5x10^5 cells were washed twice with PBS containing 2% FBS (FBS/PBS). The cells were incubated at 4˚C with a mouse anti-human c-Met MoAb (Do-24; Upstate Biotechnology, Lake Placid, NY) for 60 min. After being washed twice with FBS/PBS, they were incubated with FITC-labeled anti-mouse IgG MoAb (PharMingen), washed twice with FBS/PBS, and suspended in FBS/PBS. Thereafter, the cells were incubated with murine mAbs to human CD4 and CD25, respectively conjugated with phycoerythrin (PE) and perCP. They were analyzed by FACScan using CellQuest software (Becton-Dickinson), and positivity for c-Met was evaluated in CD4 and CD25 double positive ATLL cells.

Detection of autophosphorylation of c-Met protein. Cell lines and primary ATLL cells were incubated in the presence or absence of human recombinant HGF (Sigma). To analyze the autophosphorylation of c-Met in response to HGF treatment, cellular lysates were immunoprecipitated with c-Met-specific antibody on 10% SDS-PAGE gels, electrophoretically transferred to polyvinylidine difluoride membranes (Immobilon-P; Millipore Corp., Bedford, MA), and then analyzed for immunoreactivity with a mouse anti-human c-Met polyclonal antibody (Santa Cruz Biotechnology, Santa Cruz, CA) or antiphosphotyrosine antibody (anti-PY, 4G10), and horseradish peroxidase-conjugated sheep anti-mouse IgG (Amersham Life Science, Inc., Arlington Heights, IL) with an enhanced chemiluminescence detection system (Amersham Life Science, Inc.).

Proliferation assay. For assays of cell proliferation, IL-2-deprived KK-1 cells and primary ATLL cells were cultured at a density of 5x10^5/ml and 1x10^6/ml viable cells assessed by trypan blue staining, respectively, in 96-well flat-bottomed microtitre plates in 200 μl of RPMI-1640 medium containing 10% FBS, 2 mmol/l L-glutamine and antibiotics, with or without human recombinant HGF (Sigma), anti-human HGF Ab (R&D) or anti-human HGF R(c-Met) Ab (R&D) for 48 h, and were then mixed with MTS [3-(4,5-dimethylthiazol-2-yl)-5-(3-carboxymethoxyphenyl)-2-(4-sulfophenyl)-2H-tetrazolium, inner salt]. Cell proliferation was measured with a CellTiter 96 Aqueous One Solution Cell Proliferation Assay (Promega, Madison, WI, USA). All samples were analyzed in triplicate.

Cytokine assay. MNCs from patients with ATLL, normal individuals, or cell lines were suspended in RPMI-1640

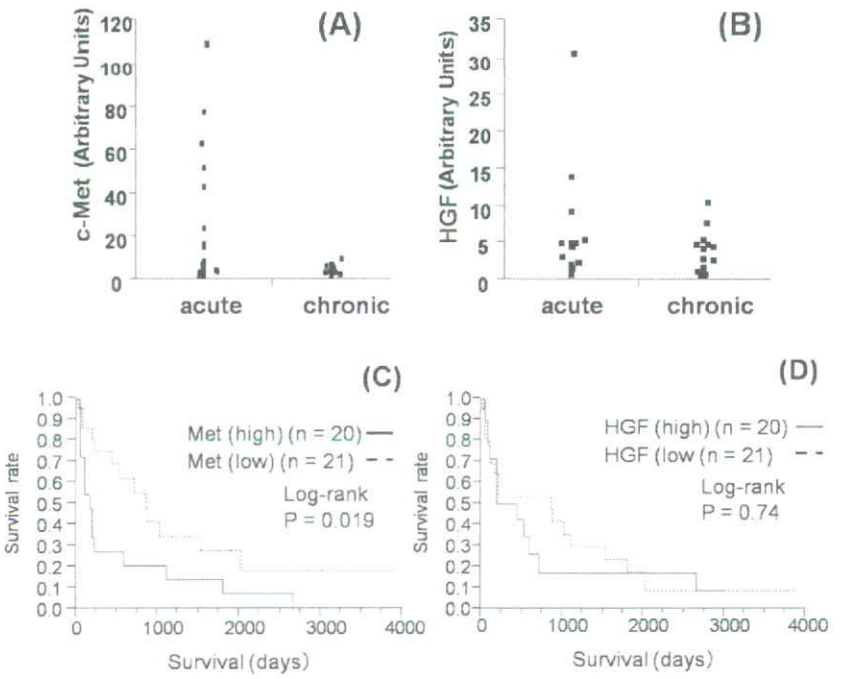

Figure 1. Expression level of c-Met but not HGF was associated with clinical subtypes of ATLL and prognosis. (A) Expression levels of c-Met and HGF by microarrays were compared between 22 acute cases and 19 chronic cases of ATLL. Leukemic CD4 positive cells from acute ATLL expressed significantly more c-Met than those from chronic ATLL (25.0 unit vs. 16.4 unit, p=0.021 by Mann-Whitney test). (B) In contrast, the difference was not significant for HGF (23.5 unit vs. 18.1, p=0.15 by Mann-Whitney test). (C) Overall survival of 41 ATLL patients in relation to c-Met expression status analyzed by microarray. (D) Overall survival of 41 ATLL patients in relation to HGF expression status analyzed by microarray.

medium containing 10% fetal bovine serum (M.A. Bioproducts, Walkersville, MD) and 200 JRM/ml IL-2 at a concentration of $5x10^5$/ml and $2x10^6$/ml viable cells assessed by trypan blue staining, respectively. After 72 h of incubation, supernatant fluid was collected for assays. We examined the concentrations of HGF and IL-6 in the plasma and the supernatant fluid samples by enzyme-linked immunosorbent assay (Quantikine; R&D).

Immunohistochemistry. Using a formalin-fixed, paraffin-embedded section of liver from autopsy specimens, we performed immunohistochemical analysis. The antibodies used were a rabbit polyclonal antibody against c-Met (SC-10, Santa Cruz Biotechnology) at 1:20 dilution and a rabbit polyclonal antibody against HGF (SC-7949, Santa Cruz Biotechnology) at 1:20 dilution (18). Tissue blocks were sectioned at 5-micron thickness and were put on coated slide glass. After deparaffinization, the sections were pretreated in pH 6.0 citrate buffer by microwave for 10 min for antigen retrieval. The tissues were incubated with 3% H_2O_2 to block unspecific reaction for 5 min. After washing with PBS, the tissue were incubated with the first antibody for 1 h in room temperature, then, washed with PBS, and were incubated with DAKO EnVision system for 30 min. The stains were visualized with DAB.

Results

Expression level of c-Met but not HGF was associated with clinical subtypes of ATLL and prognosis (Fig. 1). Expression levels of c-Met and HGF by oligonucleotide microarrays were compared between 22 acute cases and 19 chronic cases of ATLL. Leukemic CD4 positive cells from acute ATLL expressed significantly more c-Met than those from chronic ATLL. In contrast, the difference was not significant for HGF. Also, high expression of c-Met but not HGF was associated with worse overall survival.

Expression of c-Met protein in leukemic cells from ATLL patients. To examine the expression of c-Met on primary ATLL cells, FCM-based analyses were performed using PBMCs freshly isolated from ATLL patients as described previously (17). We observed the expression of c-Met on CD4 and CD25 double positive ATLL cells from 12 of 14 patients with acute-type ATLL, but none of 7 patients with chronic-type ATLL (Table I). c-Met was expressed in HUT102 and KK1, which were IL-2 independent and dependent cell lines, respectively.

Autophosphorylation of c-Met was induced in HTLV-I-positive T-cell lines and primary ATLL cells by HGF treatment. To examine whether the c-Met expressed in HTLV-I-positive ATLL cell lines and primary ATLL cells is functional, we analyzed the autophosphorylation of c-Met in response to HGF treatment. A signal of M_r 140,000 representing autophosphorylation of c-Met was detected in c-Met-positive KK-1 as described, and primary ATLL cells for the first time, when they were incubated in the presence of HGF (Fig. 2) (16). In those cells, the autophosphorylation of c-Met was not observed in the absence of HGF treatment. In contrast,

Table I. Expression of c-Met, growth response to HGF, and cytokine assay in primary ATLL cells and ATLL cell lines.

	ATLL cell line positive/tested cases	Primary ATLL cells (Chronic type) positive/tested cases	Primary ATLL cells (Acute type) positive/tested cases
Expression of c-Met	2/8	0/7	12/14
Growth response to HGF	1/2	0/7	9/11
HGF concentration (plasma)	N.A.	0/6	8/8
HGF concentration (culture[a])	2/5	2/5	6/12
IL-6 concentration (culture[a])	2/2	4/4	5/5

[a]Supernatant of short-term cultured ATLL cells. N.A., not available.

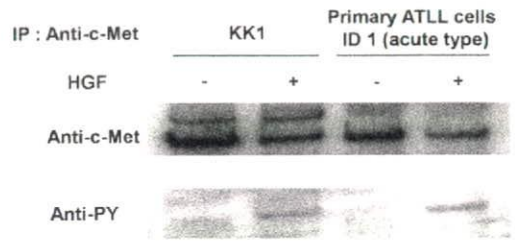

Figure 2. c-Met expressed in an HTLV-1-positive cell line and in primary ATLL cells is autophosphorylated in response to HGF. c-Met-positive KK-1 cells, and primary leukemic cells from a patient with acute ATLL were incubated in the presence (+) or absence (-) of HGF, lysed, immunoprecipitated with anti-c-Met antibody, and blotted with the same antibody or phosphotyrosine (anti-PY) antibody.

no signal representing c-Met or phosphotyrosine could be detected in c-Met-negative ATLL cell lines and primary ATLL cells (data not shown).

HGF induces ATLL cell proliferation. We next measured cell proliferation in primary ATLL cells and ATLL cell lines after stimulation with HGF. As shown in Fig. 3A, KK1, an IL-2-dependent ATLL cell line, showed a proliferative response to HGF in a dose-dependent manner after being deprived of IL-2 in contrast to c-Met negative cell lines. The response was at least partially blocked by anti-HGF or anti-c-Met antibodies (Fig. 3B). Similarly, HGF induced a proliferative response in c-Met-positive ATLL cells from 9 of the 11 acute cases with c-Met expression but not in c-Met-negative ATLL cells from 7 chronic cases (Fig. 3C).

Cytokine assay. The plasma levels of HGF in patients with ATLL are shown in Fig. 4A. The level was most elevated in acute type, and moderate in chronic type ATLL as compared to healthy individuals. Next, we analyzed HGF levels in the supernatants of short-term cultured primary ATLL cells and ATLL cell lines (Fig. 4B). In some of the patients with acute or chronic type ATLL, the cytokine level was relatively elevated as compared to healthy controls. In two (KK1 and ST1) out of 5 IL-2 dependent ATLL cell lines, the level was also relatively high.

To further analyze the mechanism of the increase in plasma HGF levels in patients with acute ATLL, cells not

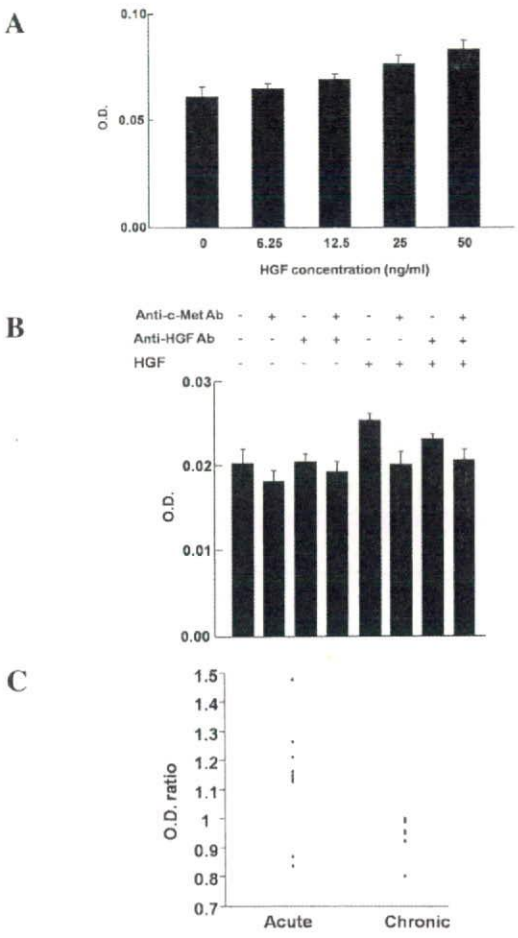

Figure 3. HGF induces proliferation of c-MET-positive cells. (A) The proliferation of c-Met-positive KK1, an IL-2 dependent ATLL cell line, was evaluated in a manner dependent on the dose of HGF after IL-2 deprival by MTS assay. Data are expressed in absorbance unit and are means ± SD of triplicates. (B) The proliferation of KK1 was evaluated in the absence or presence of HGF (50 ng/ml), alone or together with anti-HGF or anti-c-Met antibodies by MTS assay. Data are expressed in absorbance unit and are means ± SD of triplicates. (C) The proliferation of c-Met-positive ATLL cells from acute cases and that of c-Met-negative ATLL cells from chronic cases were evaluated in the presence of HGF (50 ng/ml) by MTS assay. Data are expressed as ratio of the absorbance unit with that in the absence of HGF of triplicates in each case. The difference between acute and chronic cases were significant (1.13 vs. 0.94, Mann-Whitney p=0.016). HGF induced a proliferative response (ratio >1.06) in c-Met-positive ATLL cells from 9 of the 11 acute cases but not in the c-Met-negative ATLL cells from 7 chronic cases.

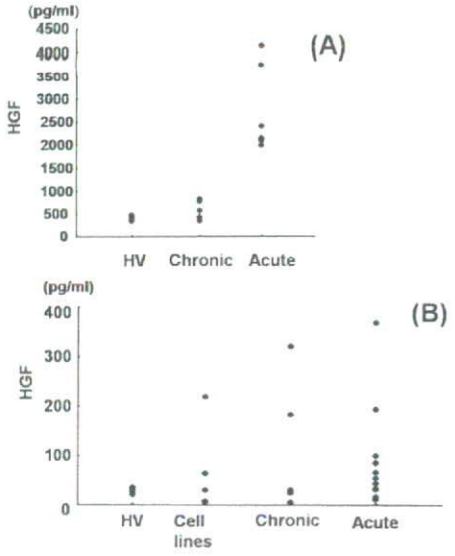

Figure 4. High level of HGF in plasma from ATLL patients and/or supernatant of short-term cultured cells from ATLL patients and HTLV-1-positive cell lines. MNCs from patients with ATLL, healthy volunteers (HV), or cell lines were cultured with IL-2. After 72 h of incubation, supernatant fluid as well as plasma was collected for assays. The concentrations of HGF in the plasma (A) and the supernatant fluid (B) samples were measured by enzyme-linked immunosorbent assay.

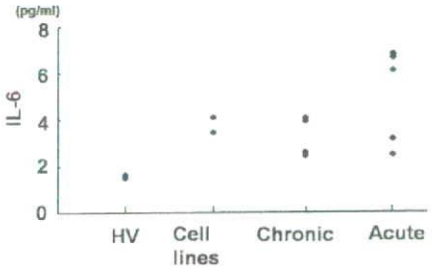

Figure 5. High level of IL-6 in supernatant of short-term cultured cells from ATLL patients and HTLV-1-positive cell lines. MNCs from patients with ATLL, healthy volunteers (HV), or cell lines were cultured with IL-2. After 72 h of incubation, supernatant fluid was collected for assays. The concentrations of IL-6 in the supernatant fluid samples were measured by enzyme-linked immunosorbent assay.

producing the cytokine *in vitro* were measured as to the concentration of IL-6, which had been reported to induce HGF production in stromal cells, in supernatant of short-term cultured ATLL cell lines and primary ATLL cells (19). The level was most elevated in acute types including cases with ATLL cells not secreting HGF, and moderate in chronic types and the cell lines as compared to healthy individuals (Fig. 5).

Immunohistochemistry. To evaluate the relationship between tissue-invasiveness and c-Met/HGF expression in ATLL, liver autopsy specimens from 2 patients suffering with liver dysfunction were analyzed. Immunostaining revealed most and some infiltrated atypical lymphocytes were c-Met-positive cells in each one case, respectively (Fig. 6). Hepatocytes

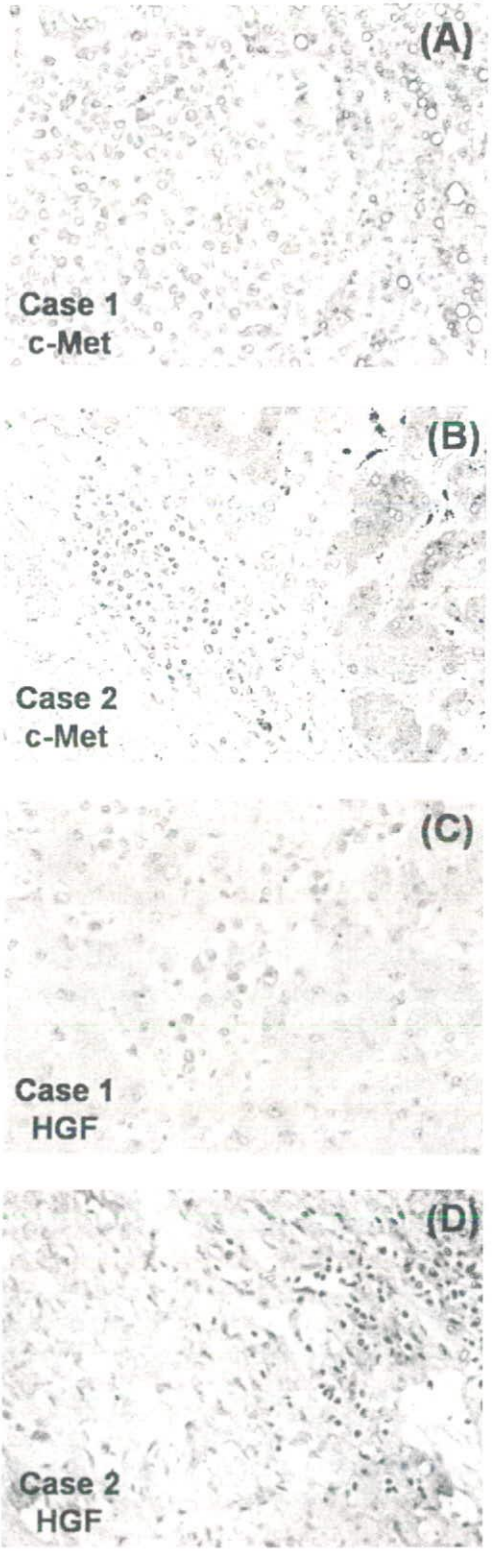

Figure 6. Immunohistochemical staining of c-Met and HGF in invasive ATLL, and adjacent normal hepatocytes and srtomal fibroblasts from patients suffering from liver dysfunction. (A and C) Case 1 showed expression of c-Met in most of infiltrating large atypical lymphocytes and that of HGF in some of the atypical cells. Hepatocytes were positive for c-Met and negative for HGF, respectively. (B and D) Case 2 showed expression of c-Met in some large atypical lymphocytes. Weak expression of HGF was shown in the cytoplasm of stromal fibroblasts but was rare in ATLL cells.

were stained weak with anti-c-Met antibody as described previously (20). In the case with c-Met expression in most atypical lymphocytes, some of the cells were also positive for HGF. In the other case, HGF was positive in most adjacent stromal fibroblasts but rare in atypical lymphocytes.

Discussion

HGF/c-Met signaling has been shown to play a significant role in promoting tumor cell invasion and metastasis in a wide variety of human tumors (10,11,13,14). We previously found that the expression level of c-Met was higher in leukemic cells of acute type than chronic type ATLL by microarray-based gene expression profiling. Furthermore, the plasma concentration of HGF was increased in most acute and some chronic cases although the expression was not significantly detected in leukemic cells by microarray and PCR (17). We also previously reported that c-Met expression in ATLL was associated with liver-invasiveness of the disease (16). Here, we studied HGF/c-Met interaction using ATLL cell lines, primary leukemic cells and liver autopsy specimens from patients with the disease to elucidate the mechanism of multi-step carcinogenesis and tissue-invasiveness.

We first compared the significance of c-Met and HGF on the clinical features of ATLL. Expression of c-Met but not HGF was increased in acute cases as compared to chronic cases and associated with poor prognosis. In contrast to HGF expression in leukemic cells, plasma HGF concentration was higher in acute cases. Collectively, both c-Met expression in leukemic cells and concentrations of HGF in plasma were increased in most patients with acute ATLL, but rare in patients with chronic ATLL.

Overexpression of HGF and/or c-Met has been reported in various human cancers. Some tumor cell-derived factors, such as IL-1, IL-6 and TNF-α, are involved in the over-expression of HGF in stromal fibroblasts (18,21). Thus, such growth factors produced in stromal cells interact with the receptors expressed on tumor cells (paracrine pattern). In addition, malignant tumor cells also frequently produce growth factors and their receptors (autocrine pattern). Therefore, the HGF/c-Met pathway plays an important role during tumor progression in a paracrine pattern and/or autocrine pattern (22,23). The levels of HGF, and/or IL-6 were elevated in the supernatant of short-term cultured ATLL cells from some patients with acute or chronic disease as well as the cell lines KK1 and ST1. Notably, the IL-6 level in the supernatant was elevated in some cases without an elevation of HGF in the supernatant. These results suggest autocrine and/or paracrine growth stimulated by HGF and c-Met in acute ATLL cells secreting HGF and/or IL-6 which induce production of HGF by stroma cells, respectively. Plasma concentrations of IL-6 in the acute cases were significantly higher than those in the chronic cases of ATLL in our previous study (24). ATLL cells as well as HTLV-1 infected cells from HTLV-1 carriers and patients with HTLV-1 associated myelopathy secrete not only IL-6 but other HGF-inducers such as IL-1ß and TNF-α, through which the production of HGF in stromal cells could be up-regulated (25-27).

The expression of c-Met in c-Met-positive ATLL cells from an acute case was functional as well as in KK1 by detecting autophosphorylation of the protein after HGF treatment. Furthermore, we showed for the first time that HGF induced the proliferation of primary ATLL cells from most c-Met-positive acute cases examined as well as the KK1 cell line in contrast to c-Met-negative cells. This effect was at least partially blocked by antibodies to HGF and c-Met in KK1. These results strongly suggest the c-Met/HGF interaction to be an important event during the acute transformation of ATLL from the chronic phase. Although the HGF concentration was elevated in supernatant of KK1 cells and plasma of the acute case, autophosphorylation of c-Met was not detected in those cells without HGF treatment possibly because the concentration was not high enough to induce autophosphorylation. Interestingly, liver dysfunction associated with ATLL invasion was detected in three of the 12 c-Met positive cases in contrast to none of the 9 negative cases in this series. In two of the cases, infiltrated ATLL cells and adjacent stromal cells in liver were shown to be positive for c-Met/HGF and HGF, respectively, suggesting the autocrine and paracrine loop. The invasion by ATLL cells of organs such as the liver could expose the cells to hypoxia and induce c-Met expression as hypothesized in invasive and metastatic cancers (10,16,28). Also, HGF concentration could be elevated at invasive lesion secreted by ATLL cells or adjacent stromal cells (18,23).

Given that the JAK-STAT signaling pathway is activated in the leukemic cells of patients with advanced ATLL (29), it may be relevant that binding sites for STAT1/STAT3 are present in the promoter regions of c-Met. The mechanism of overexpression of c-Met includes amplification of the gene (30). However, we did not detect a significant difference in DNA content at the c-Met locus between chronic and acute ATLL in our previous study (17). It is thus possible that JAK-STAT signaling contributes to the transcriptional activation of c-Met.

IL-2/IL-2R, IL-15/IL-15R and chemokine I-309 loop have been reported to induce autocrine and/or paracrine growth of aggressive ATLL cells (31-33). However, plasma levels of IL-2 and IL-15 were low in those studies. In contrast, HGF level in some acute cases were more than 4 ng/ml, which could induce some proliferation in KK1 and primary ATLL cells. Despite low plasma concentration of HGF, interestingly, the level in supernatant of short-term cultured ATLL cells from some chronic types was also elevated as acute ATLL. Although c-Met was not expressed in chronic types, the secretion of HGF by the cells after IL-2 stimulation might reflect the early phase of the transition to acute ATLL. There have been reports on several targets for the treatment of ATLL (34-37). The c-Met pathway is among drug targets in cancer progression and provides at least three avenues of selective anticancer development: antagonism of ligand/receptor interaction, inhibition of TK catalytic activity, and blockade of intracellular signaling. Human clinical trials in two of the three areas are now underway (10,11,22,23). Our study revealed that blocking the pathway might be effective against aggressive ATLL as well as solid cancers.

In conclusion, we provide the first evidence of autocrine and/or paracrine growth of primary leukemic cells and tissue-invasive cells stimulated by HGF and c-Met in aggressive ATLL secreting HGF and/or IL-6, respectively. In addition,

the c-Met/HGF system may represent a suitable target for the treatment of ATLL.

Acknowledgements

We wish to thank Mr. Masanobu Anami, M.T., C.T., at the Department of Pathology, Nagasaki University Hospital, for his excellent cooperation on immunohistochemical staining.

References

1. Uchiyama T, Yodoi J, Sagawa K, Takatsuki K and Uchino H: Adult T-cell leukemia: clinical and hematologic features of 16 cases. Blood 50: 481-492, 1977.
2. Poiesz BJ, Ruscetti FW, Gazdar AF, Bunn PA, Minna JD and Gallo RC: Detection and isolation of type C retrovirus particles from fresh and cultured lymphocytes of a patient with cutaneous T-cell lymphoma. Proc Natl Acad Sci USA 77: 7415-7419, 1980.
3. Taylor GP and Matsuoka M: Natural history of adult T-cell leukemia/lymphoma and approaches to therapy. Oncogene 24: 6047-6057, 2005.
4. Shimoyama M: Diagnostic criteria and classification of clinical subtypes of adult T-cell leukaemia-lymphoma. A report from the Lymphoma Study Group (1984-1987). Br J Haematol 79: 428-437, 1991.
5. Shimoyama M: Chemotherapy of ATL. In: Adult T-Cell Leukemia. Takatsuki K (ed). Oxford University Press, Oxford, pp221-237, 1994.
6. Pawson R, Mufti GJ and Pagliuca A: Management of adult T-cell leukaemia/lymphoma. Br J Haematol 100: 453-458, 1998.
7. Tsukasaki K, Utsunomiya A, Fukuda H, *et al*: VCAP-AMP-VECP compared with biweekly CHOP for adult T-cell leukemia-lymphoma: Japan Clinical Oncology Group Study JCOG9801. J Clin Oncol 25: 5458-5464, 2007.
8. Boros P and Miller CM: Hepatocyte growth factor: a multifunctional cytokine. Lancet 345: 293-295, 1995.
9. Furge KA, Zhang YW and Vande Woude GF: Met receptor tyrosine kinase: enhanced signaling through adapter proteins. Oncogene 19: 5582-5589, 2000.
10. Boccaccio C and Comoglio PM: Invasive growth: a MET-driven genetic programme for cancer and stem cells. Nat Rev Cancer 6: 637-645, 2006.
11. Peruzzi B and Bottaro DP: Targeting the c-Met signaling pathway in cancer. Clin Cancer Res 12: 3657-3660, 2006.
12. Beilmann M, Vande Woude GF and Dienes HP and Schirmacher P: Hepatocyte growth factor-stimulated invasiveness of monocytes. Blood 95: 3964-3969, 2000.
13. Borset M, Hjorth-Hansen H, Seidel C, Sundan A and Waage A: Hepatocyte growth factor and its receptor c-met in multiple myeloma. Blood 88: 3998-4004, 1996.
14. Capello D, Gaidano G, Gallicchio M, *et al*: The tyrosine kinase receptor met and its ligand HGF are co-expressed and functionally active in HHV-8 positive primary effusion lymphoma. Leukemia 14: 285-291, 2000.
15. Yamada Y, Kamihira S, Murata K, *et al*: Frequent hepatic involvement in adult T cell leukemia: comparison with non-Hodgkin's lymphoma. Leuk Lymphoma 26: 327-335, 1997.
16. Imaizumi Y, Murota H, Kanda S, *et al*: Expression of the c-Met proto-oncogene and its possible involvement in liver invasion in adult T-cell leukemia. Clin Cancer Res 9: 181-187, 2003.
17. Choi YL, Tsukasaki K, O'neill MC, *et al*: A genomic analysis of adult T-cell leukemia. Oncogene 47: 2163-2173, 2006.
18. Masuya D, Huang C, Liu D, *et al*: The tumour-stromal interaction between intratumoral c-Met and stromal hepatocyte growth factor associated with tumour growth and prognosis in non-small-cell lung cancer patients. Br J Cancer 90: 1555-1562, 2004.
19. Khan KN, Masuzaki H, Fujishita A, *et al*: Interleukin-6- and tumour necrosis factor alpha-mediated expression of hepatocyte growth factor by stromal cells and its involvement in the growth of endometriosis. Hum Reprod 20: 2715-2723, 2005.
20. Prat M, Narsimhan RP, Crepaldi T, Nicotra MR, Natali PG and Comoglio PM: The receptor encoded by the human c-MET oncogene is expressed in hepatocytes, epithelial cells and solid tumors. Int J Cancer 49: 323-328, 1991.
21. Nakamura T, Matsumoto K, Kiritoshi A, Tano Y and Nakamura T: Induction of hepatocyte growth factor in fibroblasts by tumor-derived factors affects invasive growth of tumor cells: *in vitro* analysis of tumor-stromal interactions. Cancer Res 57: 3305-3313, 1997.
22. Mazzone M and Comoglio PM: The Met pathway: master switch and drug target in cancer progression. FASEB J 20: 1611-1621, 2006.
23. Matsumoto K and Nakamura T: Hepatocyte growth factor and the Met system as a mediator of tumor-stromal interactions. Int J Cancer 119: 477-483, 2006.
24. Yamamura M, Yamada Y, Momita S, Kamihira S and Tomonaga M: Circulating interleukin-6 levels are elevated in adult T-cell leukaemia/lymphoma patients and correlate with adverse clinical features and survival. Br J Haematol 100: 129-134, 1998.
25. Yamada Y, Ohmoto Y, Hata T, *et al*: Features of the cytokines secreted by adult T-cell leukemia (ATL) cells. Leuk Lymphoma 21: 443-447, 1996.
26. Tendler CL, Greenberg SJ, Burton JD, *et al*: Cytokine induction in HTLV-I associated myelopathy and adult T-cell leukemia: alternate molecular mechanisms underlying retroviral pathogenesis. J Cell Biochem 46: 302-311, 1991.
27. Yamano Y, Machigashira K, Ijichi S, Usuku K, Kawabata M, Arimura K and Osame M: Alteration of cytokine levels by fosfomycin and prednisolone in spontaneous proliferation of cultured lymphocytes from patients with HTLV-I-associated myelopathy (HAM/TSP). J Neurol Sci 151: 163-167, 1997.
28. Gasparini G, Longo R, Fanelli M and Teicher BA: Combination of antiangiogenic therapy with other anticancer therapies: results, challenges, and open questions. J Clin Oncol 23: 1295-1311, 2005.
29. Migone TS, Lin JX, Cereseto A, *et al*: Constitutively activated Jak-STAT pathway in T-cells transformed with HTLV-I. Science 269: 79-81, 1995.
30. Danilkovitch-Miagkova A and Zbar B: Dysregulation of Met receptor tyrosine kinase activity in invasive tumors. J Clin Invest 109: 863-867, 2002.
31. Kukita T and Arima N: Autocrine and/or paracrine growth of adult T-cell leukaemia tumour cells by interleukin 15. Br J Haematol 119: 467-474, 2002.
32. Yamada Y, Tsukasaki K, Kamihira S, *et al*: Interleukin-15 (IL-15) can replace the IL-2 signal in IL-2-dependent adult T-cell leukemia (ATL) cell lines: expression of IL-15 receptor alpha on ATL cells. Blood 91: 4265-4272, 1998.
33. Ruckes T, Saul D, Van Snick J, Hermine O and Grassmann R: Autocrine antiapoptotic stimulation of cultured adult T-cell leukemia cells by overexpression of the chemokine I-309. Blood 98: 1150-1159, 2001.
34. Waldmann TA, Goldman CK, Bongiovanni KF, *et al*: Therapy of patients with human T-cell lymphotrophic virus I-induced adult T-cell leukemia with anti-Tac, a monoclonal antibody to the receptor for interleukin-2. Blood 72: 1805-1816, 1988.
35. Mori N, Yamada Y, Ikeda S, *et al*: Bay 11-7082 inhibits transcription factor NF-kappaB and induces apoptosis of HTLV-I-infected T-cell lines and primary adult T-cell leukemia cells. Blood 100: 1828-1834, 2002.
36. Zhang Z, Zhang M, Goldman CK, Ravetch JV and Waldmann TA: Effective therapy for a murine model of adult T-cell leukemia with the humanized anti-CD52 monoclonal antibody, Campath-1H. Cancer Res 63: 6453-6457, 2003.
37. Mori N, Matsuda T, Tadano M, *et al*: Apoptosis induced by the histone deacetylase inhibitor FR901228 in human T-cell leukemia virus type 1-infected T-cell lines and primary adult T-cell leukemia cells. J Virol 78: 4582-4590, 2004.

Int J Hematol (2008) 88:551–564
DOI 10.1007/s12185-008-0207-z

ORIGINAL ARTICLE

Adhesion-dependent growth of primary adult T cell leukemia cells with down-regulation of HTLV-I p40Tax protein: a novel in vitro model of the growth of acute ATL cells

Kazuhiro Nagai · Itsuro Jinnai · Tomoko Hata · Tetsuya Usui · Daisuke Sasaki · Kunihiro Tsukasaki · Kazuyuki Sugahara · Yoshitaka Hishikawa · Yasuaki Yamada · Yuetsu Tanaka · Takehiko Koji · Hiroyuki Mano · Shimeru Kamihira · Masao Tomonaga

Received: 28 February 2008 / Revised: 7 October 2008 / Accepted: 16 October 2008 / Published online: 2 December 2008

Abstract In order to better understand the biology of adult T cell leukemia (ATL), we aimed to establish a novel method, which allows the primary growth of ATL cells using a co-culture system with murine bone marrow-derived stromal cells, MS-5. ATL cells grew in close contact with MS-5 layers and formed so-called "cobblestone areas" (CAs) without the addition of IL-2. In clinical samples, eight of ten (80.0%) cases of acute or lymphoma type ATL cells formed CAs. The frequency of CA forming cells in ATL cells ranged from 0.03 to 1.04%. The morphology, immunophenotyping, and DNA analysis indicated that cells composing CA were compatible with ATL cells, and clonally identical to primary CD4-positive ATL cells. Furthermore, in ATL cells composing CA, the expression of p40Tax was down-regulated in transcriptional and translational level, while that of HTLV-I basic leucine zipper factor (HBZ) gene was comparable to the level of primary ATL cells, resembling expression pattern of proviral genes in in vivo ATL cells. By microarray analysis, several genes which coded products involved in cell–cell interaction, and cellular survival and proliferation, were differentially expressed in ATL cells composing CA compared with primary samples. In conclusion, our co-culture system allows for the first time the growth of primary ATL cells in vitro, and might be useful as an in vitro assay for biological and clinical studies to develop molecular targeting drugs against ATL.

Keywords Adult T cell leukemia · Microenvironment · In vitro co-culture system · Cell adhesion

K. Nagai (✉) · S. Kamihira
Transfusion Service, Nagasaki University Hospital of Medicine and Dentistry, 1-7-1 Sakamoto, Nagasaki 852-8501, Japan
e-mail: agwkn@nagasaki-u.ac.jp

I. Jinnai
Division of Hematology, Department of Internal Medicine, Saitama Medical School, Saitama, Japan

T. Hata · K. Tsukasaki · M. Tomonaga
Department of Hematology, Molecular Medicine Unit, Atomic Disease Institute, Nagasaki University Graduate School of Biomedical Sciences, Nagasaki, Japan

T. Usui · D. Sasaki · K. Sugahara · Y. Yamada · S. Kamihira
Department of Laboratory Medicine, Nagasaki University Graduate School of Biomedical Sciences, Nagasaki, Japan

Y. Hishikawa · T. Koji
Department of Histology and Cell Biology, Nagasaki University Graduate School of Biomedical Sciences, Nagasaki, Japan

Y. Tanaka
Department of Immunology, Graduate School and Faculty of Medicine, University of the Ryukyus, Okinawa, Japan

H. Mano
Division of Functional Genomics, Jichi Medical University, CREST, Japan Science and Technology Agency, Tochigi, Japan

1 Introduction

Adult T cell leukemia (ATL) is a lymphoma of mature CD4-positive T cells with frequent leukemic manifestation. Patients with ATL show variable clinical manifestations and a diverse prognosis, being classified into four subtypes; smoldering, chronic, lymphoma, and acute [1, 2]. The disease is also molecularly characterized by monoclonal integration of the provirus of human T-lymphotropic virus type 1 (HTLV-1), which has been

accepted as an etiologic agent of ATL [3, 4]. However, since only a small proportion of HTLV-I carriers develop ATL [5], and the latent period from the initial infection of HTLV-1 until the onset of this disease is over 40–60 years [2], it is believed that, in addition to HTLV-1 viral proteins, as yet undetermined multi-step accumulations of leukemogenic changes in cellular genes and dysregulation of transcription by epigenetic changes may have great roles in providing a growth advantage to the malignant clone and in the evolution to the fully aggressive phase of this neoplastic disease [6].

A few culture systems have allowed primary ATL cells to grow in vitro [7–9], although they showed only transient and cytokine-dependent proliferation. Furthermore, in these reports, it was demonstrated that once placed under in vitro culture conditions, especially when stimulated with interleukin-2 (IL-2), ATL cells began to abundantly express HTLV-1 viral protein p40Tax, a protein encoded by the pX regulatory region of the HTLV-1 genome [10]. The interactions of Tax with a number of cellular molecules, transcriptional factors or modulators of cellular functions, have been reported, resulting in the trans-activation or -repression of many specific cellular genes involved in the control of cell growth or apoptosis [11–13], and it is considered to contribute to the initial immortalization and transformation of HTLV-1-infected T lymphocytes. However, ATL cells do not produce any distinct amount of Tax proteins in vivo [3], although the expression of the *tax* gene has been detected using highly sensitive RT-PCR or RT-PCR in situ hybridization in several previous reports [14, 15]. These findings suggest that in vitro growth in cultures supported with IL-2 does not necessarily reflect the growth mechanism of ATL cells in vivo.

To address this issue, we aimed at establishing a novel method to allow the primary growth of ATL cells using a co-culture system with a stromal cell layer to provide various factors to support proliferation of target cells. Previously, using long-term cultures of stromal cells obtained from lymph nodes (LNs) of ATL patients, we observed that a number of cytokines were produced which might contribute to several clinical manifestations [16]. Thus, we have speculated that there might be some important interactions between the lymphohematopoietic microenvironment of LN or bone marrow (BM) and ATL cells. It has been demonstrated that by co-culturing with the murine BM-derived stromal cell line MS-5, it is possible to support the long-term proliferation of primitive hematopoietic progenitors, B-cell progenitor cells, and acute lymphoblastic leukemia (ALL) blasts [17, 18]. Thus, the system may be assumed to have properties by which human neoplastic lymphoid cells are able to grow without any exogenous cytokine.

Fig. 1 Characterization of cobblestone areas (CAs) formed by primary ATL cells using a co-culture system of ATL cells with a murine stroma cell line, MS-5. **a** Scheme of co-culture experiments: ATL cells from patients were cultured and observed as described in "Sect. 2". **b** Phase-contrast micrographs (×200) indicate time-course changes in CAs of primary ATL cells. ATL cells from a patient (UPN007) were cultured and observed on days 3, 7, 14, and 28, as indicated, respectively. **c** Photographs indicate representative results obtained from UPN 1; May-Giemsa staining (×600), immunostaining for CD4, and PCNA (×600), respectively, left to right. **d** Integration of HTLV-1 proviral DNA; Clonality of primary ATL cells and ATL cells composing CA of UPN001 and UPN005 was examined by SBH using whole HTLV-I probes[26]. Restriction enzyme (*EcoR*I or *Pst*I) was indicated at the bottom of the figure. *Lanes* 1 and 15: marker, 2: ST-1, 3: MS-5 co-cultured with MT-2, 4: MS-5 co-cultured with HUT-102, 5 and 11: primary ATL cells of UPN001, 6 and 12: ATL cells in CA of UPN001, 7 and 13: primary ATL cells of UPN005, 8 and 14: ATL cells in CA of UPN005, 9: HUT-102, 10: MT-2. **e** HTLV-1 proviral load was quantified using real-time PCR method to test involvement of HTLV-1 genome to MS-5 stromal layer[27]. Light and dark gray bars indicate the results of the proviral load in co-cultured MS-5 and original HTLV-1 related cell lines (MT-2 and HUT-102), respectively. **f** Comparison of capacity of CA formation in co-culture experiments with different types of stromal layer. 1×10^5 ATL cells from UPN001, 003, 005, and 010 were co-cultured with stromal layer of MS-5 (*filled diamond*), HESS-5 (*filled square*), and HUVEC (*filled triangle*), in triplicate. Culture dishes were observed daily, and the numbers of CAs were counted at days 3, 5, 7, 10, 14, and 21. Values represent the means plus or minus standard error of the mean

In the present study, primary ATL cells were co-cultured with MS-5 cells and the usefulness of this co-culture system was demonstrated also for ATL cells. The significance of this novel stroma cell-dependent in vitro clonal culture system as a new model of primary ATL cell growth will be discussed.

2 Materials and methods

2.1 Cell lines and primary ATL cells

Four human HTLV-1-infected T cell lines established from normal lymphocytes (MT-2 and HUT-102) and one IL-2-independent (OMT) and three IL-2-dependent (ST-1, KOB, and KK-1) ATL cell lines established from clinical cases were used [19]. With informed consent according to the Helsinki Declaration, clinical samples of ATL cells were obtained from 20 patients, and normal $CD4^+$ T lymphocytes were obtained from peripheral blood of two healthy volunteers. The diagnosis and subtypes of ATL were defined as described by Shimoyama et al. [20]. Mononuclear cells (MNCs) were isolated from samples by Ficoll Paque gradient centrifugation (Amersham Pharmacia Biotech. NJ). ATL cells or normal $CD4^+$ T lymphocytes were enriched by labeling with magnetic bead-conjugated anti-CD4 monoclonal antibody (CD4 MicroBead; Miltenyi Biotec, Auburn, CA, USA), and then purified through a miniMACS magnetic cell separation column (Miltenyi Biotec).

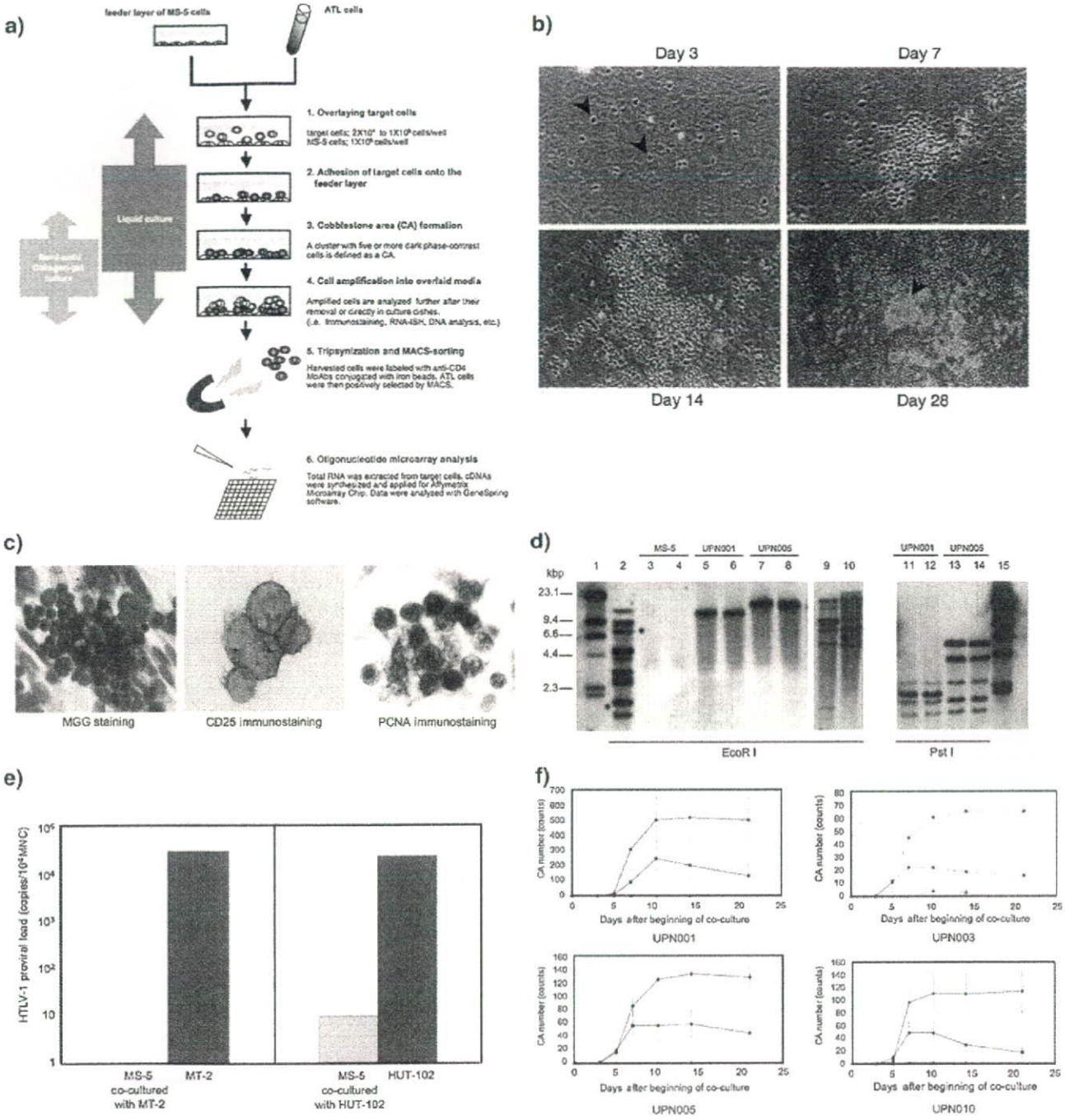

2.2 Monoclonal antibodies (MoAbs)

LT-4 (anti-p40Tax; mouse IgG_3) and Gin-7 (anti-p19Gag; mouse IgG2b) were used to detect Tax and Gag protein, respectively, by immunocytochemical staining [21, 22]. Leu3a (anti-CD4), Leu2a (anti-CD8), anti-Tac (anti-CD25), and PC-10 (anti-proliferating cell nuclear antigen (PCNA); DAKO Cytomation) were also used for immunophenotyping.

2.3 Co-culture system with a stromal layer of MS-5 cells

Murine marrow stromal MS-5 cells were kindly provided by Kirin Brewery Co. Ltd (Gunma, Japan). This cell line was originally established by Itoh et al. [17]. Maintenance of MS-5 cells and preparation of stromal feeder layers for co-culture experiments were as described previously [18]. The co-culture experiments are outlined in Fig. 1a. In short,

target cells were overlayed at various concentrations (2×10^4 to 1×10^5 cells/35 mm well) in RPMI1640 medium, including 20% fetal bovine serum (FBS), onto the feeder layer of MS-5 cells. The culture medium was changed twice a week. The culture dishes were observed daily under a phase-contrast microscope, and after an adequate period, cultured cells were processed in the following experiments.

In order to compare the capacity of target cell growth with the MS-5-stromal layer, co-culture experiments with HESS-5, which can support human hematopoietic cells in in vitro culture [23], or human umbilical venous endothelial cells (HUVEC) were performed. The murine marrow stroma cell line HESS-5 was kindly provided by the Pharmaceutical Frontier Research Laboratory, JT Inc. (Yokohama, Japan). HESS-5 cells were maintained in alpha-minimal essential medium (alpha-MEM; GIBCO) supplemented with 10% (v/v) horse serum (HS). HUVEC was purchased from Bio-Whittaker Inc., MD, USA, and maintained in accordance with the manufacturer's instructions.

In a few experiments, 2×10^5/mL ATL cells were cultured in RPMI1640 containing 20% FBS and 200 ng/mL recombinant human IL-2 (R&D systems) for five to seven days without any stromal feeder layers (liquid culture) for comparison studies with the co-culture system.

Strictly, to test the plating efficiency of primary ATL cells, we employed the Cellmatrix™ (Nitta gelatin Inc., Osaka, Japan) collagen gel culture kit according to the manufacturer's instructions. After verifying the formation of cellular clusters in a semi-solid state, these were counted under a phase-contrast microscope.

2.4 Immunocytostaining

Cells cultured on multi-chamber BioCoat/FALCON Culture Slides™ (Falcon Labware) were washed with phosphate-buffered saline (PBS). In some experiments, cytospin preparations were made from colony-composing cells and from liquid cultures. For immunostaining CD4, CD8, CD25, PCNA, and HTLV-1-related proteins, preparations were fixed with appropriate fixatives for each antigens, incubated with primary antibodies, and stained using the streptavidin–biotin-alkaline phosphatase-labeling method or the diaminobenzidine tetrahydrochloride-based horse-radish peroxidase reaction as described previously [24, 25]. To estimate the positive staining rate, a minimum of 200 ATL cells was observed under a light microscope with a final magnification of 1,000× (Nikon, Japan).

2.5 Southern blot hybridization (SBH) and HTLV-1 proviral load

The pattern of integration of the HTLV-1 provirus into the host genome was investigated using SBH as described previously [26]. In short, first, ATL cells, which proliferated in the co-culture system, were harvested by trypsinization. Cell suspension was collected from culture vessels, and subsequently left to settle for 30 min at 37°C in fresh flasks, which allowed for the separation of ATL cells from adherent MS-5 cells onto the bottom of the flasks. After harvesting the supernatant, which included many ATL cells, and MS-5 cells, separately, genomic DNA was extracted from them. Aliquots of DNA were digested with restriction enzyme of *Eco*RI or *Pst*I, and then processed for SBH using a digoxigenin-labeled whole HTLV-1.

HTLV-1 proviral load was quantified using a real-time DNA PCR LightCycler Technology System according to our previously described method [27]. The sample copy number was estimated by interpolation from the standard curve generated by serial dilution of a *tax*-containing plasmid.

2.6 Cell adhesion blockade analysis

To inhibit the adhesion of ATL cells to the MS-5 monolayer, a Cell Culture Insert™ membrane (Falcon) with 0.4 μm pore size, on which 5×10^4 target cells were overlayed in methylcellulose including 20%FBS/RPMI1640, was inserted into the 35 mm culture well with the MS-5 monolayer on the bottom of each dish. In some experiments of this setting, 20%FBS/RPMI1640 was substituted for conditioned medium (CM), which was harvested from co-culturing of MT-2 and MS-5 layer.

2.7 RNA in situ hybridization (ISH)

The mRNA expression of the HTLV-I *tax* gene was investigated by ISH using a synthetic single-stranded 40-base oligonucleotide probe corresponding to 7409-7453 of this genetic region. The sequences of the oligo-DNA probes were as follows [28]: antisense probe for *tax* mRNA: 3′-ACGCCCTACTGGCCACCTGTCCAGAGCATCAGA TCACCTG-5′, sense probe for *tax* mRNA: 3′-TGCG GGATGACCGGTGGACAGGTCTCGTAGTCTAGTGG AC-5′, and antisense probe for 28S ribosomal RNA as an internal control: 3′-TGCTACTACCACCAAGATCTGCA CCTGCGGCGGC-5′. These probes were conjugated with digoxigenin (DIG) at 3′. Unstained cytospin preparations and cultured chamber-slides were fixed for 10 min in 2% paraformaldehyde/PBS at room temperature. Subsequently, fixed preparations were processed using the Ventana HX Discovery™ (Ventana Medical Systems, Tucson, AZ) automated ISH instrument system according to the manufacturer's instructions. The conditions of each reaction were as follows: denaturation; for 10 min at 42 °C for 10 min, hybridization with oligo-probe; for 6 h at 37 °C, incubation with secondary antibody; for 30 min at 37 °C, and

colorization in streptavidin-conjugated HRP solution; for 90 min at 37 °C. The expression of the Tax gene was evaluated using a light microscope (Nikon, Japan) with a final magnification of 1,000×. A minimum of 200 ATL cells was observed in each specimen to estimate the positive staining rate. ATL cells were considered to have expressed the Tax gene when they displayed a blue–gray signal in their cytoplasm or nucleus.

2.8 Oligonucleotide microarray analysis

$CD4^+$ ATL cells were harvested from the co-culture system by trypsinization, and purified by MACS magnetic cell separation system (Miltenyi Biotec) immediately. Primary samples were also processed as described above, except for trypsinization. Enrichment of the $CD4^+$ fraction was evaluated by subjecting portions of MNC and $CD4^+$ cell preparations to analysis of the expression of CD4 by flow cytometry (FACSCaliber™; Becton-Dickinson, Mountain View, CA, USA). In all samples, the $CD4^+$ fraction constituted greater than 90% of the eluate of the affinity column. Total RNA was isolated from CD4-positive ATL cells using TRIzol reagent as described by the manufacturer (Life Technologies, Inc., Gaithersberg, MD), and then treated with RNase-free DNase I (RQ1 DNase) at 37 °C for 30 min (Promega, Madison, WI). The preparation of RNA and hybridization with HGU133A & B microarrays (Affymetrix, Santa Clara, CA, USA) were as described previously [29].

2.9 Quantification of mRNA levels using real-time PCR

Total RNA was used for cDNA synthesis using Oligo(dT)12–18 Primer (Invitrogen) and SuperScript TM3 Reverse Transcriptase (Invitrogen). Real-time PCR (*Taq*-Man) analysis was performed on a LightCycler (Roche) according to the manufacturer's instructions. Primers used for the validation studies of expression profiles are shown in Table 3. Experiments were performed with triplicates for each sample, and the glyceraldehydes-3 phosphate dehydrogenase (GAPDH) expression was used to normalize the expression of each gene for sample-to-sample differences in RNA input, RNA quality and reverse transcriptase efficiency. Furthermore, quantification of mRNA levels of HTLV-I basic leucine zipper factor (HBZ) and Tax genes was performed as described previously [30]. Assays were carried out in duplicate and the average value was used as absolute amounts of HBZ and Tax mRNA in samples.

2.10 Statistical analysis

The Mann–Whitney *U* test and Student's *t* test were used for statistical analysis with StatView software. To analyze the data of microarray analysis, the fluorescence intensity of each gene was normalized relative to the median fluorescence value for all human genes with a "Present" and "Marginal" call (Microarray Suite; Affymetrix) in each hybridization. Comparative analysis by fold change data was performed with GeneSpring 7.0 software (Silicon Genetics, Redwood, CA, USA).

3 Results

3.1 Growth of ATL cells in co-culture system with MS-5

HTLV-1-transformed and ATL patient-derived cell lines grew in close contact with the stromal layer of MS-5 cells and formed so-called "cobblestone areas" (CAs), which were made up of dark-contrasted clusters of growing cells under phase-contrast microscopy [31], without any exogenous cytokines. Not only IL-2-independent cell lines (MT-2, HUT-102, and OMT), but also two of three IL-2-dependent cell lines in our series, ST-1 and KOB, formed CAs without the addition of IL-2. KK-1 showed minimal growth in this culture system without IL-2.

Next, ATL cells from clinical samples were also used in this co-culture system. In representative cases, which showed prosperous growth, ATL cells adhered and crept into the stromal layer in a few days from the start of co-culture, grew with formation of CAs from day 10 to 14, and continued to grow over three weeks and proliferated upward into the medium out of CA cells in the third or fourth week of co-culture (Fig. 1b). In eight of 10 (80.0%) samples of acute ATL and one sample of lymphoma type, CA formation was observed, whereas three samples from two patients with chronic type of ATL, one with smoldering type and the control peripheral T cells obtained from healthy volunteers with Con-A stimulation did not have CA-forming cells (Table 1).

In May-Grunwald-Giemsa (MGG) staining, growing cells in CAs showed small lymphocyte-type morphology with convoluted nuclei as primary ATL cells show, although some growing cells showed immature, namely blastic features, which differed from primary malignant cells in the peripheral blood obtained from the patients. Immunostaining of CD4 and CD8 revealed that these cells had the immunophenotype of helper T cells, which were identical to primary ATL cells. Furthermore, since PCNA immunostaining in CA-composing cells from ATL showed a positive reaction, these cells were assumed to be in a growth phase (Fig. 1c). In two cases (UPN001 and 005), SBH analysis revealed that the integration pattern of the HTLV-1 provirus in ATL cells composing CA in each case was identical to that in primary ATL cells (Fig. 1d).

Table 1 Proliferation assay of primary ATL cells co-cultured with MS-5 cells

UPN	Subtype	Material	Frequency of clonogenic cells (%)		
			CAFC	Colony formation	
				IL-2 (+)[a]	IL-2 (–)
001	Acute	PE	1.04	0	0
		PB	0.78	0	0
002	Acute	PB	0	0	0
003	Acute	LN	0.32	0	0
004	Acute	PB	0.03	0	0
		LN	0.05	0	0
005	Acute	PB	0.12	0	0
006	Acute	PB	0.08	0	0
007	Acute	PB	0.25	0	0
008	Acute	LN	0.31	0	0
009	Acute	PB	0	0	0
010	Acute	LN	0.25	0	0
011	Lymphoma	LN	0.68	0	0
012	Chronic	PB	0	0.034	0
013	Chronic	PB	0	0.012	0
014	Chronic	PB	0.014	0.031	0
015	Smoldering	PB	0	0	0
016	Healthy[b]	PB	0	nd	nd
017	Healthy[b]	PB	0.008	nd	nd

PB peripheral blood, *LN* lymph node, *PE* pleural effusion

[a] Concentration of IL-2 was 200 ng/ml

[b] Con-A-stimulated (10 ng/ml) T cells were cultured

Table 2 Inhibitory effect of contact between ATL cells and stromal layer of MS-5

Sample	Frequency of clonogenic cells (%)						
	CAFC		Colony formation				
MS-5 stroma	+	+	+	+	+	–	–
Contact inhibition[a]	–	–	+	+	+	–	–
Co-cultured CM[b]	–	–	–	+	–	+	–
Exogenous IL-2[c]	–	+	–	–	+	–	+
UPN005 (acute)	0.12	0.21	0	0	0	0	0
UPN006 (acute)	0.08	0.06	0	0	0	0	0
UPN007 (acute)	0.25	0.24	0	0	0	0	0
UPN009 (chronic)	0	0.08	0	0.08	0	0	0.08

[a] A CellCulture Insert™ membrane was inserted to the co-culture system to inhibit direct cell–cell interaction between ATL cells and MS-5 cell layer. Values represent frequency of CAFC or colony-forming unit in the co-culture system and in the co-culture system with contact inhibition or in conditions without a MS-5 layer, respectively

[b] In this condition, we added conditioned medium (CM) which was harvested from co-culturing of MT-2 and MS-5 layer

[c] Concentration of IL-2 was 200 ng/ml

3.2 Significance of adhesion of ATL cells to stromal layer

A contact-inhibition experiment with a Cell Culture Insert™ membrane inserted in culture dishes was performed for four cases (three cases of acute type and one case of chronic type). In all three acute cases, CAs formed only under conditions, which allowed for close contact with the stromal layer of MS-5 cells. There was no colony formation in methylcellulose semi-solid cultures under contact inhibition to the stromal layer using Cell Culture Insert™, or without a stromal layer, regardless of stimulation by exogenous IL-2 or co-cultured CM. In a chronic subtype, although there was no CA formation in this co-culture system, colony formation was observed with IL-2 stimulation (Table 2). SBH analysis and quantification studies of HTLV-1 viral load revealed that infection of HTLV-1 to MS-5 cells was not detected in co-culturing with MT-2, although slightly detected in co-culturing with HUT-102 (Fig. 1d, e).

Compared with the MS-5 stromal layer, significantly less CA formed in co-culture with the HESS-5 stromal layer after day 7 of co-culturing, although we could observe comparable adhesion and growth of target cells on both stromal layers at earlier phase. Furthermore, there was no sustainable CA formation in co-culture with HUVEC (Fig. 1f). We applied the co-culture system with the MS-5 stromal layer in further analysis because of its superior efficiency for CA formation.

The semi-solid collagen gel culture of five primary ATL samples [UPN001 (PB), 003, 005, 007, and 011] revealed a linear relationship between the inoculated cell number and CA count, indicating that this assay system would be useful to quantify clonogenic precursors of ATL cells, i.e., CA-forming cells (CAFC) (Fig. 2a; Table 1). In our series, the frequency of CAFC in acute or lymphoma type varied considerably, ranging from 0.03 to 1.04% (median 0.25), and was significantly higher than in chronic type or healthy donors ($P < 0.01$; Fig. 2b).

3.3 HTLV-1 proviral gene expression in neoplastic CAs

The production of Tax and Gag proteins in ATL cells co-cultured with a stromal layer were examined by immunostaining and ISH. Based on immunostaining, these proteins seemed to disappear in CAs in ATL cell lines, HUT-102 and ST-1 (Fig. 3a).

Four cases of acute-type ATL showed a strong staining pattern for these proteins in primary neoplastic cells after liquid culture with stimulation by IL-2; however, ATL cells in CA showed significantly weaker staining for Tax and Gag proteins in all four cases (Fig. 3b). Furthermore, in

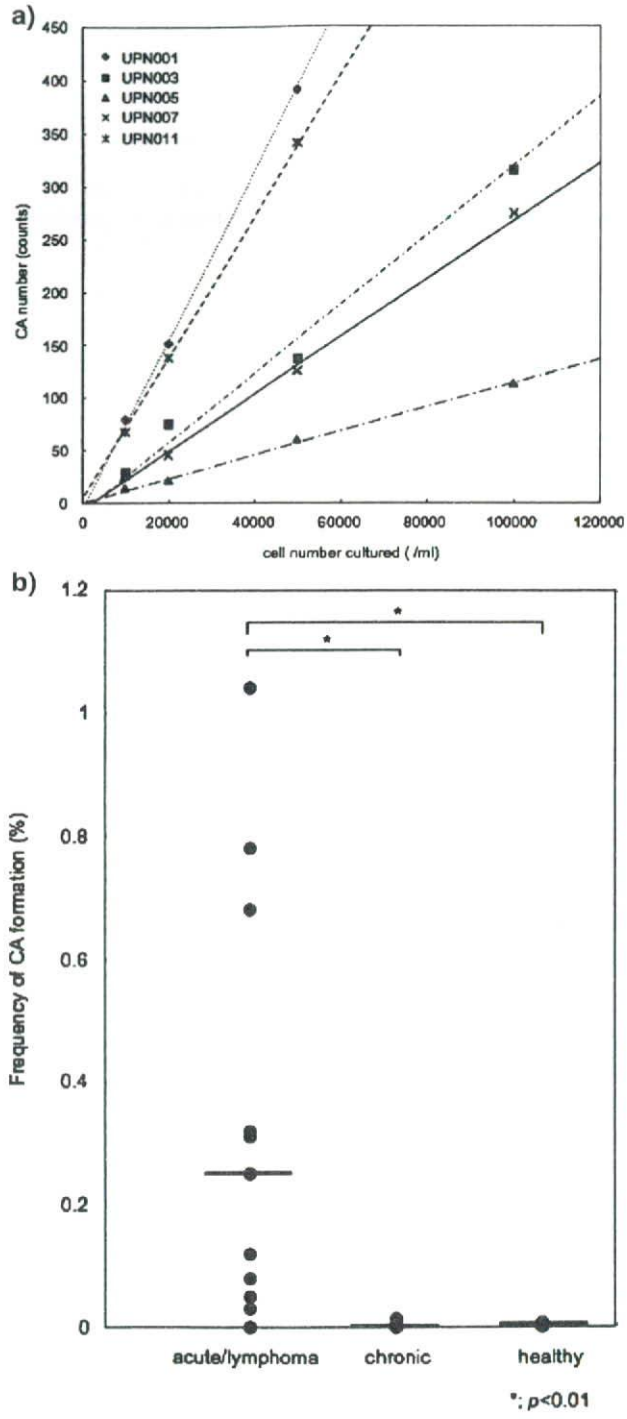

Fig. 2 Plating efficiency of ATL cells in a co-culture system with MS-5 cells. **a** The frequency of CA-forming cells (CAFC) of five cases (UPN001 (PB), 003, 005, 007, and 011) was examined with semi-solid collagen gel in the co-culture system. A clear linear relationship was obtained between the inoculated cell number and CAFCs in all cases examined. **b** The distribution plots of frequency of CA formation in different sample group; There is statistical difference in the median (*horizontal bars*) among acute/lymphoma type (0.25%), chronic type (0%), and healthy volunteers (0.04%) ($P < 0.01$)

three cases of acute ATL, the results of ISH revealed that the expression of the Tax gene of ATL cells in CA was markedly decreased when compared with that of growing cells in liquid culture with IL-2 (Fig. 3c).

Next, we quantified the expression level of HBZ gene, which was recently identified in the 3′-LTR of the complementary sequence of HTLV-1 and has been suggested as a critical gene in leukemogenesis of ATL [6, 32, 33]. As shown in Fig. 3d, the HBZ gene was highly expressed in MT-2 cells in CA, and the level of mRNA load was equivalent to those without co-culturing. With regard to *tax* gene, the expression level was significantly higher in cells in liquid culture without stroma than in cells in CA, although the difference was not so striking as observed in RNA-ISH analysis. Moreover, in the contact-inhibited condition to the stromal layer, the expression levels of these two genes were comparable to those without co-culturing.

3.4 Gene expression profiles of ATL cells composing CA

Next, we compared the gene expression profiles of sets of ATL cells composing CA matched with their corresponding $CD4^+$ primary samples from the same individuals by high-density oligonucleotide microarray analysis, to search for candidates of disease-specific molecules and signaling pathways, which contribute to the mechanism of adhesion-dependent proliferation in our co-culture system. After removal of transcriptionally silent genes from the analysis of 44,764 probe sets using Microarray Suite software, Student's t test ($P < 0.001$) was then used to extract genes, the expression level of which significantly differed between cells in CA and primary samples. Genes were considered up- or down-regulated if each value and the average fold change were 3.5 or greater in all three data sets. Finally, we could identify 110 and 98 genes significantly up- and down-regulated in ATL cells in CA compared with primary samples by selecting genes based on the reproducibility, respectively (Fig. 4a).

To validate the microarray findings, we performed RTQ-PCR for eight genes that were significantly up- or down-regulated in ATL cells in CA of three-paired array samples, and with code products correlating with adhesion molecules and cell–cell interaction or with cellular apoptosis and proliferation. All experiments were performed in triplicate. Variance among triplicates was less than 5%. Standard curves with correlation coefficiency greater than 0.970 were produced from the data for each gene, indicating the large dynamic range and accuracy of RTQ-PCR (data not shown). As shown in Table 3 and Fig. 4b, we confirmed that these genes were actually up- or down-regulated in ATL cells in CA, compared with primary

neoplastic cells as indicated in the microarray data. Up-regulated genes, *CDH11* [34], *Twist1* [35] and *Cav-1* [36], are considered to play a major role in tumor promotion, progression, survival and metastasis in several neoplasias. Furthermore, the down-regulation of several genes, *hCdc14A* [37], *CUGBP2* [38], *HBP1* [39], and *ZNFN1A1* [40], the products of which are recognized to play a role in suppressing carcinogenesis through various signaling pathways, were also confirmed in ATL cells in CA.

4 Discussion

In the present study, we established a new ATL cell/murine stroma cell co-culture system with which we could observe the proliferation of primary ATL cells without any additional growth factor. In previous studies, primary ATL cells were able to grow in a liquid culture containing IL-2; however, they showed only a transient and cytokine-dependent proliferation [8–10]. On the other hand, we also observed involvement of HTLV-1 genome to patients' LN stroma cells and production of several cytokines from them [16]. In the present study, infection of HTLV-1 to MS-5 was considered to be dispensable to adhesion-dependent ATL cell growth, as shown in the negative or minimal viral load in co-cultured MS-5 cells. Furthermore, since many murine cytokines cannot affect human cells [41], and especially in this co-culture system, any soluble factor or co-cultured CM did not stimulate ATL cells growth in the contact-inhibition test, direct adhesion of target cells to the stromal layer of MS-5 layers are considered to be essential for CA formation by primary ATL cells in this co-culture system.

In the lymphohematopoietic microenvironment, normal and neoplastic lymphoid cells are affected by various molecules [42, 43]. Concerning lymphoid malignancies, recent reports has indicated that interactions between neoplastic cells and BM or LN stromal cells regulate growth, survival, and homing in multiple myeloma, mantle cell lymphoma, and other non-Hodgkin lymphoma [44, 45]. Whereas, the expression of various adhesion molecules and chemokine receptors on leukemic cells, also in ATL, is assumed to be essential to the pathophysiology of this disease [46–50], the significance of these molecules in the growth and survival of ATL cells is still poorly understood. Thus, extensive investigation of the molecular interaction between neoplastic cells and lymphohematopoietic microenvironment is essential to clarify not only adhesion and transmigration, but also the growth and survival mechanism of primary ATL cells in this co-culture system.

In the present study, two murine stromal cell lines, MS-5 and HESS-5 showed significant supportive capacity on leukemic CA formation comparing with HUVEC, and also indicated their differential abilities for support of growth and survival of target cells. Both of them were originally established from C3H/HeN strain mice and might share common characters concerning the interaction between hematopoietic cells and stroma layer through integrin family members [51, 52]. Furthermore, target cells could adhere and start to grow on both stromal layers in our series. Our limited studies did not reveal the mechanism of differential abilities to support the growth of ATL cells between MS-5 and HESS-5 with respect to the direct interaction to target cells for the maintenance of CA formation. Previous reports concerning successful xeno-transplantation of ATL cells into immunodeficient mice indicated that indispensable extrinsic elements might be supplied to human neoplastic cells in these in vivo animal models sharing similarity with human lymphohematopoietic microenvironment [53, 54]. In analogy, our in vitro

Fig. 3 Expression of HTLV-1-related genes in ATL cells in CA. ▶ **a** HUT-102 and ST-1 cells were examined by phase-contrast micrographs (final magnification ×400), May-Giemsa staining (final magnification ×600), and immunostaining of Tax protein on ATL cells in CA and on cells after liquid culture using anti p40Tax antibody, Lt-4 (final magnification ×400). **b** Expression of HTLV-1 viral proteins on ATL cells in CA obtained from primary ATL cells. Four patients with acute-type ATL were examined. *Color* photographs show representative results of immunostaining of Tax (*upper*) and Gag (*lower*) in primary cells after culture with IL-2 for 7 days (*left*) and ATL cells in CA (*right*) (UPN004). *Bar graphs* are a summary of results of immunostaining of Tax and Gag protein in four cases. Light and *dark gray bars* indicate the results of primary ATL cells after liquid culture with IL-2 and those of ATL cells in CA in our co-culture system, respectively. Data are presented as the mean percentage of positive cells in triplicate experiments with error bars indicating 1SD. Mann–Whitney's *U* test was performed for statistical analysis and, in every sample, the positive rate of immunostaining of p19 and p40 was significantly lower in ATL cells in CA than in primary ATL cells after liquid culture with IL-2 ($P < 0.01$). **c** *tax* mRNA expression in ATL cells in CA obtained from primary ATL cells. ATL cells obtained from three cases were analyzed by RNA-ISH method. *Color* photographs show representative results of the analysis of UPN001; primary ATL cells after liquid culture with IL-2 (*left*) and ATL cells in CA (*right*): tested with the probe to 28S ribosomal RNA as an internal control (*upper*), the antisense oligonucleotide probe to the *tax* mRNA (*middle*), and the sense oligonucleotide probe (*lower*), indicated in "Sect. 2". Areas surrounded by arrowheads are CAs. *Bar graphs* are a summary of the results of three primary samples, which were analyzed RNA-ISH for *tax* mRNA. Light and dark gray bars indicate the results of primary ATL cells after liquid culture with IL-2 and those of ATL cells in CA in our co-culture system, respectively. Data are presented as the mean percentage of positive cells in triplicate experiments with error bars indicating 1SD. Mann–Whitney's *U* test was performed for statistical analysis and, in every sample, the positive rate of *tax* mRNA expression was significantly lower in ATL cells in CA than in primary ATL cells after liquid culture with IL-2 ($P < 0.01$). **d** Results of quantification of mRNA load of HBZ and *tax* genes. The copy number of target mRNA per 50 ng total RNA was estimated from the standard curves [29]. *Light* and *dark gray* and *white bars* indicate data, which were obtained from HUT-102 and MT-2 cell lines in three different culture conditions; conventional liquid culture, co-culture with MS-5, and contact-inhibited condition to MS-5 stromal layer, respectively

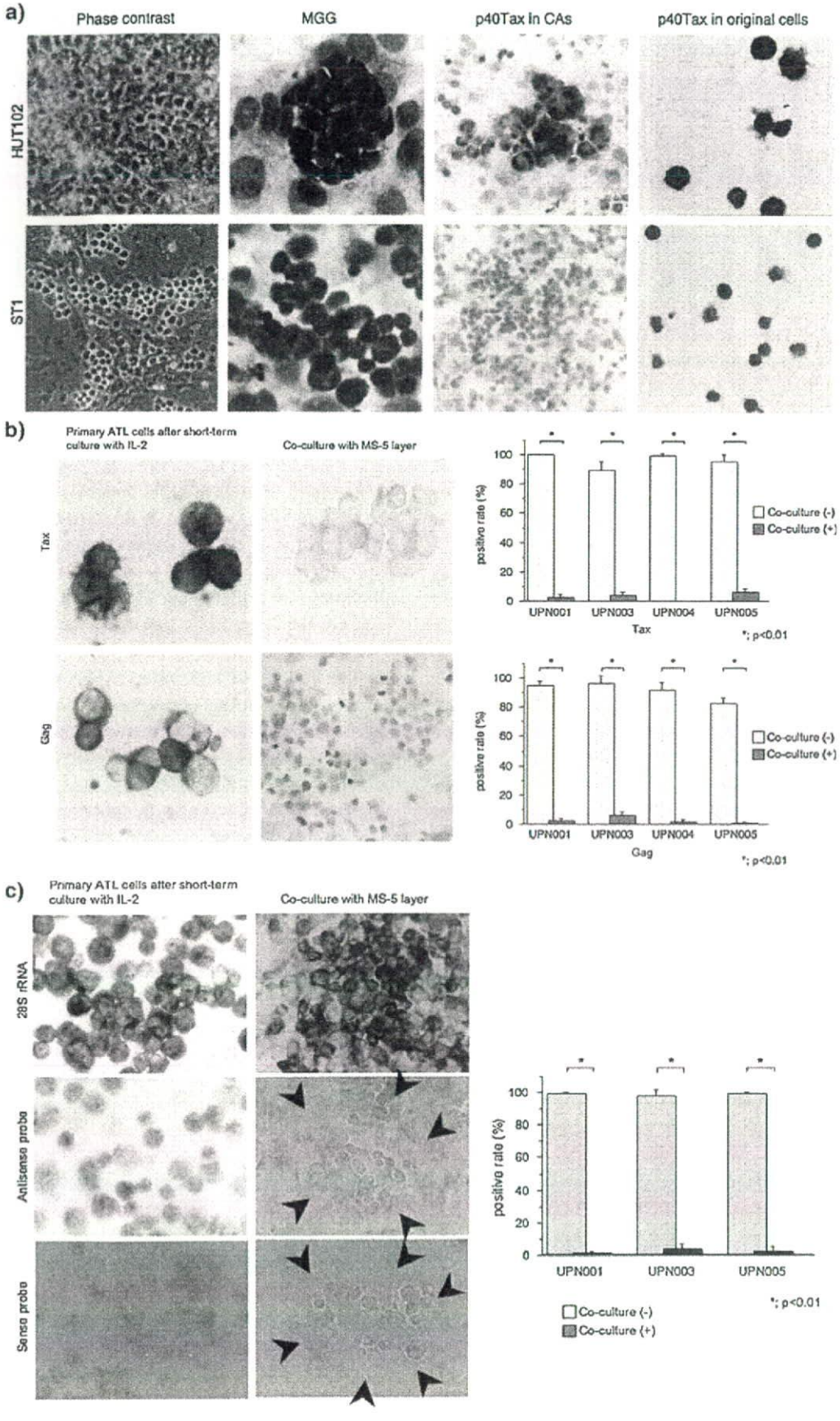
a)
Phase contrast
MGG
p40Tax in CAs
p40Tax in original cells
HUT102
ST1
b)
Primary ATL cells after short-term culture with IL-2
Co-culture with MS-5 layer
Tax
Gag
positive rate (%)
Co-culture (-)
Co-culture (+)
UPN001
UPN003
UPN004
UPN005
Tax
Gag
*; p<0.01
c)
Primary ATL cells after short-term culture with IL-2
Co-culture with MS-5 layer
28S rRNA
Antisense probe
Sense probe
positive rate (%)
UPN001
UPN003
UPN005
Co-culture (-)
Co-culture (+)
*; p<0.01